Molecular Biology of the Cell
Vol. 16, 1026–1042, March 2005

# Identification of Cell Cycle-regulated Genes in Fission Yeast[D]

**Xu Peng,*† R. Krishna Murthy Karuturi,*† Lance D. Miller,* Kui Lin,*‡ Yonghui Jia,* Pinar Kondu,§ Long Wang,* Lim-Soon Wong,‖ Edison T. Liu,* Mohan K. Balasubramanian,¶# and Jianhua Liu*@**

*Genome Institute of Singapore, Singapore 138672, Singapore; §Bioinformatics Institute, Singapore 138671, Singapore; ‖Institute for Infocomm Research, Singapore 119613, Singapore; ¶Temasek Life Sciences Laboratory, 1 Research Link, NUS, Singapore 117604, Singapore; and Departments of #Biological Sciences and @Biochemistry, National University of Singapore, Singapore 117597, Singapore

Submitted April 10, 2004; Accepted December 2, 2004
Monitoring Editor: John Pringle

**Cell cycle progression is both regulated and accompanied by periodic changes in the expression levels of a large number of genes. To investigate cell cycle-regulated transcriptional programs in the fission yeast *Schizosaccharomyces pombe*, we developed a whole-genome oligonucleotide-based DNA microarray. Microarray analysis of both wild-type and *cdc25* mutant cell cultures was performed to identify transcripts whose levels oscillated during the cell cycle. Using an unsupervised algorithm, we identified 747 genes that met the criteria for cell cycle-regulated expression. Peaks of gene expression were found to be distributed throughout the entire cell cycle. Furthermore, we found that four promoter motifs exhibited strong association with cell cycle phase-specific expression. Examination of the regulation of MCB motif-containing genes through the perturbation of DNA synthesis control/MCB-binding factor (DSC/MBF)-mediated transcription in arrested synchronous *cdc10* mutant cell cultures revealed a subset of functional targets of the DSC/MBF transcription factor complex, as well as certain gene promoter requirements. Finally, we compared our data with those for the budding yeast *Saccharomyces cerevisiae* and found ~140 genes that are cell cycle regulated in both yeasts, suggesting that these genes may play an evolutionarily conserved role in regulation of cell cycle-specific processes. Our complete data sets are available at http://giscompute.gis.a-star.edu.sg/~gisljh/CDC.**

## INTRODUCTION

The mitotic cell cycle of eukaryotic cells is a complex biological process in which many cellular events are carried out in a sequential manner to ensure precise duplication and faithful segregation of essential components into daughter cells. Cell cycle progression is thus regulated by a wide range of mechanisms such as protein modification, targeted proteolytic degradation, and cell cycle-specific transcription, which has been found to play a pivotal role in controlling cell cycle progression (Maqbool *et al*., 2003). In the budding yeast *Saccharomyces cerevisiae*, among a total of ~6000 genes, ~400–800 have been found whose transcript levels oscillate during the mitotic cell cycle (Cho *et al*., 1998; Spellman *et al*., 1998). In a human cancer cell line (HeLa), >1000 transcripts were found whose levels exhibited periodic changes during the cell cycle (Cho *et al*., 2001; Whitfield *et al*., 2002). Genes whose expression levels peak at specific stages of the cell cycle are often required for regulation of the processes that occur at these stages (Futcher, 2000).

This article was published online ahead of print in *MBC in Press* (http://www.molbiolcell.org/cgi/doi/10.1091/mbc.E04–04–0299) on December 22, 2004.

[D] The online version of this article contains supplemental material at *MBC Online* (http://www.molbiolcell.org).

† These authors contributed equally to this work.

‡ Present address: Beijing Normal University, Beijing, China.

Address correspondence to: Jianhua Liu (liujh@gis.a-star.edu.sg).

The fission yeast *Schizosaccharomyces pombe* has been an excellent model for the study of mechanisms regulating the eukaryotic cell cycle (Nurse, 1990). As in other eukaryotic cells, the fission yeast cell cycle can be divided into four discrete phases: G1, S, G2, and M (Mitchison, 1970). A primary characteristic of the G1 phase is the synthesis and accumulation of active proteins required for DNA replication in the subsequent S phase, during which an entire complement of chromosomal DNA is synthesized. In rapidly growing fission yeast, the G1 and S phases are relatively short, each occupying ~10% of the cell cycle (Nasmyth *et al*., 1979). After S phase, cells enter G2, which is the lengthiest phase and occupies ~70% of the cell cycle. Increase of cell mass in wild-type cells occurs largely in G2 under exponential growth conditions. On reaching a critical cell mass and/or cell volume, cells progress into M phase, which is marked by chromosome condensation, formation of the mitotic spindle, and the segregation of chromosomes to opposite ends of the cells (Robinow, 1977; Hagan and Hyams, 1988). After nuclear division, cytokinesis occurs associated with the formation of a medial division septum that is then partially digested to physically separate the two daughter cells. Because the M, G1, and S phases typically occur before physical separation of the daughter cells, newborn fission yeast cells have typically already entered early G2 phase (MacNeill and Fantes, 1997).

About 40 of the 4970 genes in the *S. pombe* genome (Wood *et al*., 2002) had been reported previously to display cell cycle-regulated transcription (Table 2). Some of these genes

**Table 1.** *S. pombe* strains used in this study

| Strain | Relevant genotype | Comment |
|---|---|---|
| JLY1497 | *leu1-32 h*$^{-[\rho]}$ | Laboratory stock |
| JLY188 | *leu-32 ura4-D18 h*$^{-[\rho]}$ | Laboratory stock |
| JLY1537 | *cdc2-22 leu-32 ura4-D18 h* | Laboratory stock |
| JLY275 | *cdc10-V50 leu-32 ura4-D18 h*$^{-[\rho]}$ | Laboratory stock |
| JLY1603 | Δ*ace2::ura4*$^{+}$ *leu-32 ura4-D18 h*$^{-[\rho]}$ | See text |
| GC187 | *cdc10-C4 leu-32 h*$^{-[\rho]}$ | McInerny *et al*., 1995 |
| 2–843 | Δ*sep1::ura4*$^{+}$ *ura4-D18 h*$^{-[\rho]}$ | Ribár *et al*., 1997; laboratory stock |

contain MCB consensus sequences in their promoters. It has been shown that DNA synthesis control (DSC) transcriptional complexes (also known as MCB-binding factors, or MBF) can bind MCB motifs and activate transcription of genes that are required for the G1/S transition (Whitehall *et al*., 1999). The DSC complexes contain the products of the genes *cdc10*, *res1*, *res2*, *rep1*, and *rep2* (Lowndes *et al*., 1992; Caligiuri and Beach, 1993; Miyamoto *et al*., 1994; Sugiyama *et al*., 1994; Zhu *et al*., 1994; Nakashima *et al*., 1995; White *et al*., 2001). Recently, another transcriptional complex, named the *pombe* cell cycle box (PCB)-binding factor (PBF), has been proposed to regulate cell cycle-specific transcription that peaks at the M-G1 boundary (Anderson *et al*., 2002). Although the composition of the PBF complex is not clear, it has been shown that it binds to PCB consensus sequences and regulates transcription activities in a Plo1p-dependent manner (Anderson *et al*., 2002). Many genes have been identified that contain PCB promoter consensus motifs and exhibit an expression peak at the M-G1 interval (Anderson *et al*., 2002). These include *cdc15* (Fankhauser *et al*., 1995); *fin1* (Krien *et al*., 2002); and *mid1*, *plo1*, *sid2*, and two genes previously characterized as G1-S genes, *mcm2* and *ppb1*. Expression of three genes (*cdc25*, *rum1*, and *wis3*) has been shown to peak in the G2 phase (Ducommun *et al*., 1990; Benito *et al*., 1998; Samuel *et al*., 2000).

Although a number of studies have focused on the expression of individual genes that function in various cell cycle-regulatory processes, a systematic approach had not been applied to study expression of all genes through the cell cycle. We report here a genome-wide analysis of cell cycle-regulated transcription in *S. pombe* by using synchronous cultures generated by two different techniques and an oligonucleotide-based DNA microarray representing >99% of the open reading frames (ORFs) in the annotated genome. We have identified many cell cycle-regulated genes and used this set of genes to identify the promoter elements that may control their expression. We have also studied the extent of evolutionary conservation of cell cycle-regulated transcription by comparing our results to those obtained with *S. cerevisiae*. The primary data sets presented in this article can be found at http://giscompute.gis.a-star.edu.sg/~gisljh/CDC.

## MATERIALS AND METHODS

### Strains and Media

The strains used in this study are listed in Table 1. Cells were cultured in YES medium (0.5% yeast extract, 3.0% glucose, 225 mg/l uracil and leucine) at the temperatures indicated. *ace2* deletion strain JLY1063 was constructed in strain JLY188 by using a polymerase chain reaction (PCR)-mediated approach (Bähler *et al*., 1998) with *ura4*$^{+}$ as the selective marker. The deletion allele in strain JLY1603 was validated by PCR by using sequence-specific primer pairs (our unpublished data).

### Microarray Manufacture

Based on the annotated fission yeast genome (Wood *et al*., 2002), we used a cDNA-specific oligonucleotide selection algorithm (Lin *et al*., 2004) to select two unique 50-mer sequences for each of 4929 ORFs (>99% of the ORFs in the genome). In brief, 50-mer sequences were first selected from ORF sequences based on a set of criteria that included GC content of 45–65%, no inverted repeat of more than five consecutive nucleotides, no single nucleotide run of >11 consecutive nucleotides, and no more than 50% of the same nucleotide. ORF-specific oligonucleotides were then selected to have no more than 68% similarity to other ORF sequences in the genome to ensure ORF specificity, a criterion more stringent than the maximum allowable similarity of 75% estimated by others (Kane *et al*., 2000). More than 99% of the oligonucleotides selected were <1 kb from the 3′ end of the ORF. All the oligos were synthesized (Proligo, Hamburg, Germany), resuspended in 0.3× SSC buffer, and subsequently spotted onto poly-lysine–coated glass slides by using a spotting machine (GeneMachines, San Carlos, CA). Spotted glass slides were postprocessed according to DeRisi's protocol (http://derisilab.ucsf.edu/microarray/protocols.html) and used directly in hybridization or stored at room temperature in a dry cabinet for later use.

### Nuclear Staining and Fluorescence-activated Cell Sorting (FACS) Analysis

To stain nuclei, 1-ml culture samples were collected and fixed either by the addition of 100 μl of concentrated formaldehyde (Sigma-Aldrich, St. Louis, MO) or by brief centrifugation followed by the addition of 1 ml of cold 70% ethanol. Fixed cells were washed twice with phosphate-buffered saline buffer and stained with 4,6-diamidino-2-phenylindole (Sigma-Aldrich) to visualize nuclear DNA. For each sample, at least 500 cells were scored using a fluorescence microscope (Leica, Wetzlar, Germany).

To analyze DNA content, cells were collected by brief centrifugation and fixed by resuspension in ice-cold 70% ethanol and then treated overnight with RNase A in 50 mM sodium citrate buffer, pH 7.0. After staining with propidium iodine, the fluorescence intensities of individual cells were measured by flow cytometry using a BD FACScan (BD Biosciences, Franklin Lakes, NJ).

### Synchronization

For size-based synchronization, cells from 10 liters of early log phase culture were sonicated briefly and then subjected to elutriation centrifugation (Beckman Coulter, Fullerton, CA) at 8–10°C and 3000–4000 rpm with a constant flow rate of 100 ml/min. Synchronized wild-type cells (composed of newborn cells at early G2 phase) were grown at 30°C, and samples were collected every 10 min for a period of 6 h. Synchronized wild-type and *cdc10-V50* mutant cells also were released to 36°C and sampled every 15 min for 5 h. Cell samples were centrifuged at 2500 rpm for 2 min, and the pellets were chilled in liquid nitrogen and stored at −80°C for RNA extraction later.

Temperature-sensitive *cdc25-22* mutant cells were synchronized using the block-and-release method (Mitchison *et al*., 1991). Early log phase cells growing at 24°C were shifted to the restrictive temperature of 36°C for 4 h. The culture was then shifted back to 24°C to start synchronous growth. Samples were taken at 10-min intervals as described above.

### RNA Preparation, cDNA Fluorescence Labeling, and Microarray Hybridization

Acid phenol was added to the frozen cell pellets, which were then incubated at 65°C for 15 min with occasional shaking using a thermomixer (Eppendorf, Hamburg, Germany). The aqueous phase was recovered by centrifuging at 5000 rpm for 5 min at 4°C and reextracted using phenol:chloroform (1:1). RNA was precipitated by adding an equal volume of isopropanol and recovered by centrifugation at 10,000 rpm for 20 min at 4°C. Fluorescence-labeled cDNA was synthesized using a SuperScript II kit (Invitrogen, Carlsbad, CA) according to the manufacturer's instructions, by using oligo$(dT)_{20}$ in the presence of either Cy5- or Cy3-coupled dUTP. The reaction was stopped by the addition of EDTA, and the cDNA was briefly hydrolyzed by adding

NaOH and subsequently neutralized by adding HCl. Neutralized fluorescent cDNA was washed and concentrated using a microcon-YM30 spin-column (Millipore, Billerica, MA).

Spotted microarray slides were prehybridized using Roche hybridization buffer (Cat. no.: 1603588, Roche Diagnostics, Basel, Switzerland) with a raised coverslip (Erie Scientific, Portsmouth, NH) in a slide hybridization chamber (GeneMachines) for ~1 h at 42°C. Slides were washed first in distilled $H_2O$ for 2 min, then in isopropanol for 2 min, and finally spin-dried. Slides were then hybridized using Roche hybridization buffer containing Cy5-labeled (samples from the synchronous cultures) and Cy3-labeled (asynchronous-culture reference samples) cDNA overnight at 42°C. Hybridized slides were washed consecutively in 2× SSC/0.1% SDS for 1 min, 1× SSC for 4 min, 0.2× SSC for 4 min, and 0.05× SSC for 1 min, and then spin-dried before scanning.

## *Data Acquisition and Processing*

Microarray slides were scanned using a GenePix scanner (Axon Instruments, Union City, CA) at wavelengths of 635 and 532 nm and a resolution of 10 $\mu$m by using GenePix Pro3 or Pro4 software (Axon Instruments). GenePix Results files were generated by the program and subsequently normalized based on a median of ratios. To ensure well measured data, the ratio for a spot was collected if its intensity in either channel was twofold or greater than that of the background.

To detect cell cycle-regulated genes, we used a modified Fourier-transform method. This algorithm can be applied even with little or no prior knowledge of cell cycle-regulated genes, and it has been shown to be competitive with supervised methods by using *S. cerevisiae* and HeLa cell cycle data (Karuturi and Liu, 2004). This algorithm is described briefly below as a sequence of steps.

***Filling Missing Values.*** A missing value was replaced by the average of the values of its immediate neighbors. If one of the neighbors did not exist or also had its value missing, then the missing value was replaced by the average of the average value of the whole profile and the value of the nonmissing neighbor. These filling steps were carried out repeatedly until all the missing values were filled for each profile. This step was required for the algorithm to effectively retrieve true positives even in the presence of missing values in their profiles, because missing values would reduce the support for retrieval of genes. Filling the missing values aided in proper clustering of genes and robust estimations of peaks and phases of gene expression. As shown below, in our data, only 0.95 and 3.75% of all profiles had more than four missing values in the *cdc25* data and elutriation data, respectively; moreover, of the 747 genes predicted to be cell cycle regulated, no genes in the *cdc25* data and only 11 genes in the elutriation data had more than four missing values in their profiles. We filtered out all profiles that had missing values for more than half of the time-course length. This filtering resulted in the removal of one gene from the *cdc25* data and ~16 genes from the elutriation data.

***Gaussian Smoothing.*** The value $F_{ix}$ (expression of gene $i$ at time $t = x$) was replaced by

$$\sum_t F_{it} e^{-(t-x)^2/(2\sigma^2)}$$

where $\sigma$ was set to be equal to 1/20 of the cell cycle period. This step was performed to remove the high-frequency noise in the profiles that could otherwise affect the cell division cycle (CDC) score that we describe below. This choice of $\sigma$ ensures that it will not introduce any artificial oscillation of period close to the cell cycle period.

***Zero-Mean Local Normalization.*** Normalizing the time-course profile $F_i$ of gene $i$ such that its mean is zero is common practice. But the expression profile of a gene may have an additive linear component apart from the periodic component (Rifkin and Kim, 2002), which must be removed for a better estimate of the Fourier transform of the periodic component. We achieved this using local normalization by replacing $F_{it}$ by $(F_{it} - m_{it})$, where

$$m_{it} = \frac{1}{n_t}\sum_{x=0}^{T} F_{ix} \quad \text{if } 0 \le t < T/2\,,$$

$$m_{it} = \frac{1}{n_t}\sum_{x=t-T/2}^{t+T/2} F_{ix} \quad \text{if } T/2 \le t \le \Im - T/2\,,$$

$$m_{it} = \frac{1}{n_t}\sum_{x=\Im-T}^{\Im} F_{ix} \quad \text{if } \Im - T/2 < t \le \Im$$

in which $\Im$ and $T$ are the total profile period and the cell cycle period, respectively, and $n_t$ is the number of values being averaged. $m_{it}$ represents the local mean of profile $i$ at time $t$. This step removes the additive linear component (represented by $at+c$, where $a$, $t$, and $c$ are the rate of change of the component, time, and average expression, respectively), based on the fact that the average of values of a linear function symmetrically sampled around point $t = x$ is $ax + c$, whereas it is 0 for the function

$$\cos\left(\frac{2\pi t}{T} - \theta\right)$$

if the period of averaging is $T$ (the period of oscillation). Thus, the above-mentioned method calculates the local mean of the profile over a symmetric window of CDC period and subtracts it from the original profile value. The first and third equations take care of the border cases arising because our expression profiles are of finite length.

***Fourier Transform.*** The Fourier transform is a method for finding the peak and phase of expression of a set of cell cycle-regulated genes by using their time-course profiles. We determined the periodicity of the profile $F_i$ by fitting it with the function $P_i\cos(\omega t\text{-}\phi_i)$, in which $P_i$ is the peak value, $\omega = 2\pi/T$, and $\phi_i$ is the phase of expression. Both $P_i$ and $\phi_i$ could be estimated by finding the coefficients $A_i$ and $B_i$ of the Fourier transform of the expression profile $F_i$, as follows:

$$A_i = \sum_t \cos(\omega t) F_{it} \qquad B_i = \sum_t \sin(\omega t) F_{it}$$

$P_i$ and $\phi_i$ were then calculated as follows:

$$P_i = \sqrt{A_i^2 + B_i^2} \qquad \phi_i = \tan^{-1}(B_i/A_i)$$

These formulae assume that $\cos(\omega t)$ and $\sin(\omega t)$ are orthogonal over the duration of the profile, which may be violated if the number of cycles for which $F_i$ is generated is not equal to an integral multiple of half cycles or sampling is at irregular intervals. In such cases, $P_i$ and $\phi_i$ exhibit variation with the actual phase of $F_i$. To overcome this artifact, we introduced two corrective steps, as follows. First, after estimating $\phi_i$, we searched for the phase $\theta$ of $\cos(\omega t - \theta)$, which gave rise to the calculated phase if it were sampled at exactly the same time points as that of $F_i$. Then, the value of $\phi_i$ was replaced by that of $\theta$. Second, after correcting for phase, the calculated peak was divided by the peak obtained for $\cos(\omega t - \theta)$ if it were sampled at the same time points as that of $F_i$. Hereafter, $P_i$ and $\phi_i$ represent the corrected peak and phase of expression of gene $i$.

***CDC Score.*** Spellman *et al*. (1998) obtained the "CDC score" for each gene by multiplying its estimated peak of expression (as obtained from the Fourier transform; $P_i$ in the above-mentioned formulations) by the highest correlation value obtained between the data series for that gene and the expression profiles for known genes with peaks in the $G_1$, S, $G_2$, M, or $M/G_1$ phase. This strategy was also followed by Whitfield *et al*. (2002). However, in the unsupervised approach, peak correlation is not available. Hence, we defined two factors called mean square error and sign similarity for $F_i$ as follows:

Mean square error

$$(E_i) = (1/N)\sum_t (F_{it} - P_i\cos(\omega t - \phi_i))^2$$

where $N$ is the number of time points in the profile. $E_i$ measures how much the model deviates from the original expression profile and helps to reduce the false discovery rate.

Sign similarity

$$(C_i) = (1/N)\sum_t (W_{i(t-1)} + 1)M_{it}$$

where $M_{it} = 1$ if $F_{it}\cos(\omega t - \phi_i) > 0$ and 0 if $F_{it}\cos(\omega t - \phi_i) \le 0$, $W_{it}$ is the maximum of 0 and $(W_{i(t-1)} + \Delta(2M_{it} - 1))$ in which $W_{it} = 0$ if $t \le 0$. $\Delta$ is an increment and was set to 0.1. $M_{ik}$ indicates the agreement (takes a value of 1) or disagreement (takes a value of 0) of directionality between the profile and its model at $t = k$, and $W_{it}$ is a measure of nonrandom occurrence of $M_{ik} = 1$ for $0 \le k \le t$. $C_i$ helps to deal with noise as well as deviation from the sinusoidal shape, and it thus improves the rate of true positives.

The CDC score of gene $i$ was then defined as follows:

$$S_i = P_i C_i^{\alpha} E_i^{-\beta}$$

where $\alpha$ and $\beta$ are positive numbers that were set to 1.0 and 0.25, respectively, based on the optimum performance with the *S. cerevisiae* cell cycle data (Spellman *et al*., 1998). These settings also were found to be optimal with the human cell cycle data (Whitfield *et al*., 2002).

***Combining CDC Scores.*** The genes with the top 500 CDC scores in each data set were compared, and those present in both sets were used to calculate the average phase difference between the experiments. It was found that the wild-type elutriation experiment lagged behind the *cdc25*-mutant experiment

by 0.27 rad, which was then added to the estimated phase of all genes in the *cdc25* experiment. Then, the scores for each gene were combined to get a final score using the formula

$$^{2}\sqrt{S_{cdc25}^2 + S_{Wt}^2 + 2S_{cdc25}S_{Wt}\cos(\phi_{cdc25} - \phi_{Wt})}$$

where

$$S_{cdc25},\ S_{Wt} \text{ and } \phi_{cdc25}\ ,\ \phi_{Wt}$$

are the scores and phases of gene expression in the *cdc25* and the wild-type experiments, respectively.

### *Estimating False Discovery Rate (FDR)*

The FDR was estimated using randomly generated data. For a given list of the top $N$ (based on CDC score), transcripts whose minimum CDC score was $S_{min}$, the FDR was estimated as the number of random profiles that had CDC score $> S_{min}$ divided by $N$. The random data were generated by shuffling either the whole data set or each profile individually. The FDR reported is the greater of the two estimates, because the FDR estimates for our algorithm are robust to the randomization procedure used, as shown elsewhere (Karuturi and Liu, 2004).

### *Identification of Cell Cycle-specific Promoter Motifs*

Promoter sequences were extracted from intergenic regions (maximum of 1 kb) located immediately upstream of the start codons of the ORFs based on the published *S. pombe* genome sequence (Wood *et al.*, 2002). For the 747 genes identified, 733 promoter sequences were available and therefore analyzed. The promoter motifs listed in the *S. cerevisiae* Promoter Database at http://cgsigma.cshl.org/jian/were tested for their cell cycle phase specificity in *S. pombe*. All motifs that occurred in >300 genes were deleted from the analysis. The genes were then numbered in order of their average phase of expression. A method described by Tang and Lewontin (1999) was applied to search for cell cycle phases that were enriched for the motif-containing genes based on the ordered gene list. For the phase-specific motifs, the relative density of occurrence (fraction of motif-containing genes in a window of 100 genes divided by the average occurrence of the motif in all 733 genes) was plotted (Figure 2A).

### *Analysis of DSC-dependent or -independent Transcription*

Cells bearing the temperature-sensitive *cdc10-V50* allele were used to analyze DSC-dependent or -independent transcription. The *cdc10-V50* and wild-type control cultures were synchronized by elutriation at a permissive temperature and then shifted to 36°C. Samples were collected at 15-min intervals for 4.5 h beginning 30 min after the temperature shift. The expression profiles were analyzed using the algorithm described above. We considered the expression ratios from time point 1 to time point 8 of the *cdc10* culture and from all time points of the wild-type culture. The cell cycle periods of the *cdc10* and elutriation data were taken to be those that minimized the FDR among the top 500 genes based on CDC score and were set to 180 and 135 min, respectively. The peak (i.e., $P_{wt}$ for wild-type and $P_{cdc10}$ for *cdc10*) and CDC score (i.e., $S_{wt}$ and $S_{cdc10}$) of each gene were determined. The *cdc10* or DSC dependence score ($SD_{cdc10}$) of each gene was then calculated as follows: $SD_{cdc10} = (S_{wt}/S_{cdc10})(P_{wt}/P_{cdc10})$. Thus, a higher score means a greater DSC dependence. This approach was tested using four known DSC-dependent and seven DSC-independent genes (our unpublished data), which proved to be well separated; the seven DSC-independent genes had rank >408 (among the 4929 genes), whereas the four DSC-dependent genes had rank ≤158 (three with rank <51 and one with rank 158). Based on their $SD_{cdc10}$ scores, these same 11 genes ranked (among the 747 cell cycle-regulated genes) as follows: the seven DSC-independent genes had rank >108 and the four DSC-dependent genes had ranks ≤50 (three with rank below 23 and one with rank 50).

### *Statistical Analyses*

To test the statistical significance of the occurrence of motifs in the promoters of a given cluster of $n$ genes among a total of $N$ genes, we used binomial analysis, as follows. Let $p$ and $k$ be the fraction of the $N$ genes and the number of the $n$ genes, respectively, that have the given motif. Then, the probability of having $\geq k$ occurrences of the motif among the $n$ genes can be expressed as

$$P(r \geq k) = \sum_{r=k}^{n} \frac{n!}{(n-r)!r!} p^r (1-p)^{n-r}$$

To test the statistical significance of finding cell cycle regulation in common between *S. pombe* genes and their *S. cerevisiae* orthologues, we conducted simulations assuming that the orthologue map between the two yeasts is accurate and complete. We chose 747 and 800 genes at random from the *S. pombe* and the *S. cerevisiae* genomes, respectively, and ascertained the number of orthologues. We repeated this analysis $10^6$ times and found that the chance occurrence of ≥139 *S. pombe* genes being in the *S. cerevisiae* set was $<10^{-6}$. The converse analysis showed that the chance of ≥142 genes from that *S. cerevisiae* set having orthologues in the *S. pombe* set was also $<10^{-6}$.

To test the statistical significance of finding overlapping phases of peak expression for orthologous gene pairs, we proceeded as follows. The observed distribution is the distribution of 194 orthologue pairs among the 25 pairs of *S. pombe* and *S. cerevisiae* phases (i.e., G1, S, G2, G2/M, and M from each organism). The expected distribution is the distribution of orthologue pairs into phase pairs as calculated using the distribution of the orthologue pairs into the various phases in the respective organisms. The expected number of pairs in a phase pair (a and b) is calculated as 194PaPb, where Pa and Pb are the fractions of orthologue pairs having phase a in *S. pombe* and phase b in *S. cerevisiae*, respectively. The two distributions were considered to be indepen-

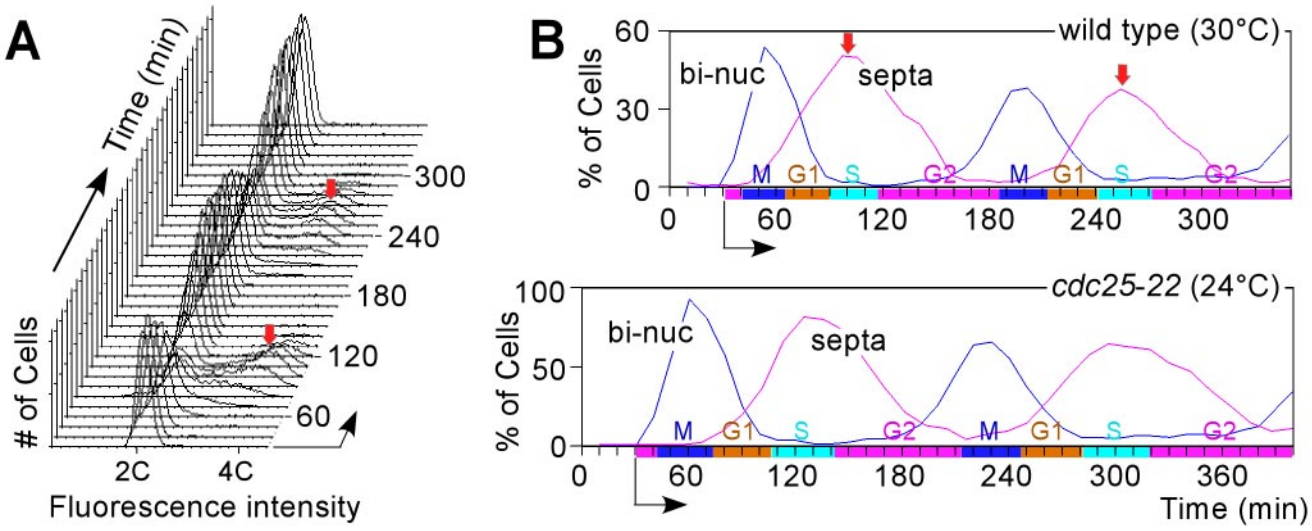


**Figure 1.** Characterization of the synchronous cultures. (A) FACS analysis of a synchronous wild-type culture. For each time point, 10,000 propidium iodine-stained cells were measured for fluorescence intensity. 2C indicates the DNA content of an interphase cell containing a G2 nucleus or a mitotic cell containing two G1 nuclei. 4C indicates the DNA content of a septated cell containing two G2 nuclei. (B) Mitotic (binucleate-cell) and septation indexes of synchronous cultures of wild-type (top) and *cdc25–22* (bottom) cells. Black arrows, start times for the samples analyzed; red arrows, times of coincident peaks of 4C cells and septated cells in the wild-type culture; colored bars, cell cycle phases.

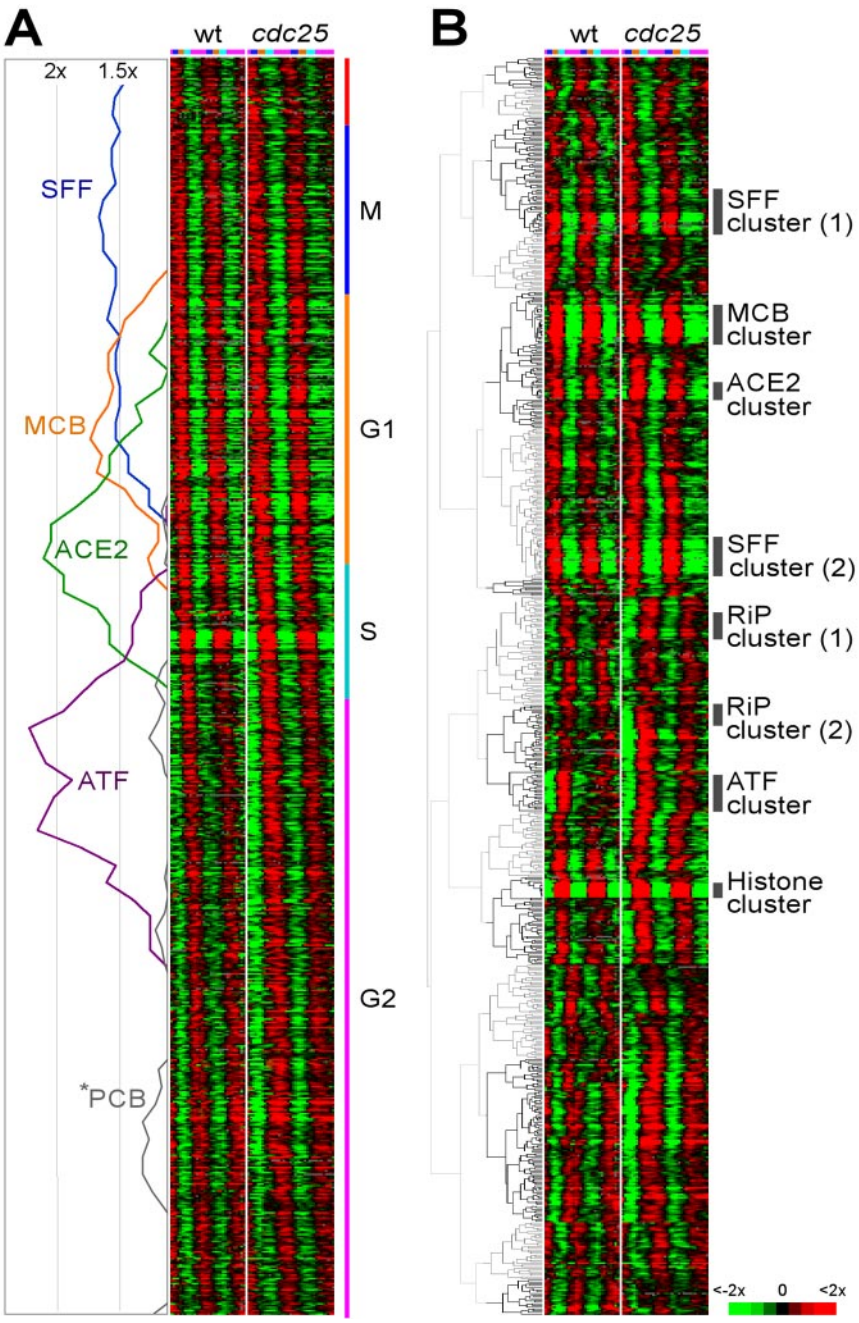


**Figure 2.** The expression profiles of 747 cell cycle-regulated genes in *S. pombe*. Genes correspond to the rows, and the time points (10-min intervals) in each experiment form the columns. The intensities of the colors indicate the magnitudes of induction (red) or repression (green) for each gene (see key at bottom right). Black, no change of expression levels; gray, data not available. The color bars on top indicate the cell cycle phases according to Figure 1. (A) Genes are ordered by their times of peak expression; phases of peak expression are indicated by the colored bars on the right. The graph on the left shows the distributions of promoter motifs indicated as densities relative to the background density for that motif (see *Materials and Methods*). The distribution of the PCB motif (asterisk) was not significantly enriched at any stage of the cell cycle. (B) Genes that share similar expression profiles are grouped by cluster analysis as described in the text. The dendrogram on the left shows the structures of the clusters; the bars on the right indicate sets of genes sharing the indicated promoter motifs.

dent to test (by $\chi^2$ test) whether the observed distribution shows any strong relationship between phase assignments in the two organisms.

## RESULTS

### *Synchronous Cultures and Cell Cycle Phases*

The sensitivity for detecting periodic transcriptional events depends largely on the degree of synchrony of the cell cultures. We used two methods of synchronization. First, by elutriation centrifugation (see *Materials and Methods*), we physically selected small-sized or newborn daughter cells at early G2 phase to initiate synchronous wild-type cell cultures. Second, we used a block-and-release approach with a *cdc25-22* temperature-sensitive mutant to generate cultures synchronized at the G2/M boundary (Mitchison *et al*., 1991). In both cases, samples were taken at 10-min intervals for a period of 6–7 h to ensure that at least two complete cell cycles were covered. Cellular DNA contents were analyzed by FACS. Either a 2C peak or both 2C and 4C peaks were observed in both wild-type (Figure 1A) and *cdc25* mutant (our unpublished data) cultures. The 4C peak represents cells that contained two G2 nuclei separated by a division septum, a consequence of the daughter cells having completed G1 and S phases before physical separation. Thus, almost all newborn daughter cells were in early G2 phase. The synchrony of both types of cultures also was assessed by measuring the percentages of binucleate cells and septum-containing cells at each time point (Figure 1B). The peaks of binucleate cells indicate synchronous mitosis, whereas the

**Table 2.** *Previously known cell cycle-regulated genes in S. pombe*

| Symbol | Systematic name | Published phase | Reference | Data from this study: Assigned phase[a] | Data from this study: CDC rank[a] |
|---|---|---|---|---|---|
| *ams2* | SPCC290.04 | M-G1 | Chen *et al.*, 2003 | G1 | 45 |
| *cdc15* | SPAC20G8.05c | M-G1 | Fankhauser *et al.*, 1995; Anderson *et al.*, 2002 | M | 57 |
| *cdc18* | SPBC14C8.07c | G1-S | Kelly *et al.*, 1993; Tanaka and Russell, 2001 | G1 | 28 |
| *cdc22* | SPAC1F7.05 | G1-S | Hofmann and Beach, 1994; Muzi-Falconi and Kelly, 1995; Ng *et al.*, 2001 | G1 | 2 |
| *cdc25* | SPAC24H6.05 | G2 | Ducommun *et al.*, 1990 | G2 | 166 |
| *cdt1* | SPBC428.18 | G1 | Hofmann and Beach, 1994 | G1 | 44 |
| *cdt2* | SPAC17H9.19c | G1-S | Hofmann and Beach, 1994; Maqbool *et al.*, 2003 | G1 | 40 |
| *cig2* | SPAPB2B4.03 | G1-S | Obara-Ishihara and Okayama, 1994 | G1 | 18 |
| *cmk1* | SPACUNK12.02c | S | Rasmussen, 2000 | NMD | * |
| *cmk2* | SPAC23A1.06c | M-G1 | Alemany *et al.*, 2002 | NMD | (1279) |
| *cnp1* | SPBC1105.17 | M-G1 | Takahashi *et al.*, 2000 | G1 | 419 |
| *dfp1* | SPCC550.13 | G1-S | Brown and Kelly, 1999; Takeda *et al.*, 1999 | G1 | 104 |
| *fin1* | SPAC19E9.02 | M-G1 | Krien *et al.*, 2002; Anderson *et al.*, 2002 | G1 | 125 |
| *grt1* | SPBPB8B6.04c | M | Yamada *et al.*, 2000 | NI | |
| histones | 9 ORFs | S | Matsumoto and Yanagida, 1985; Choe *et al.*, 1985 | S | 4–34 |
| *mcm2* | SPBC4.04c | M-G1 | Anderson *et al.*, 2002 | NMD | (2268) |
| *mid1* | SPCC4B3.15 | M-G1 | Anderson *et al.*, 2002 | G2 | 708 |
| *mik1* | SPBC660.14 | S | Christensen *et al.*, 2000 | S | 29 |
| *mrc1* | SPAC694.06c | S | Tanaka and Russell, 2001 | S | 37 |
| *pfh1* | SPBC887.14c | G1-S | Tanaka *et al.*, 2002 | G1 | 181 |
| *pht1* | SPBC11B10.10c | | Carr *et al.*, 1994 | NMD | * |
| *plo1* | SPAC23C11.16 | M-G1 | Anderson *et al.*, 2002 | M | 94 |
| *ppb1* | SPBP4H10.04 | M-G1 | Plochocka-Zulinska *et al.*, 1995; Anderson *et al.*, 2002 | NMD | * |
| *rad21* | SPCC338.17c | G1-S | Birkenbihl and Subramani, 1995 | G1 | 46 |
| *rep2* | SPBC2F12.11c | Not G1 | Nakashima *et al.*, 1995 | M | 221 |
| *res2* | SPAC22F3.09c | G1-S | Obara-Ishihara and Okayama, 1994 | NMD | * |
| *rum1* | SPBC32F12.09 | G2 | Benito *et al.*, 1998 | G1 | 649 |
| *sep1* | SPBC4C3.12 | Septation | Ribár *et al.*, 1999 | G2 | 746 |
| *sid2* | SPAC24B11.11c | M-G1 | Anderson *et al.*, 2002 | G1 | 72 |
| *slp1* | SPAC821.08c | M | Yamada *et al.*, 2000 | M | 21 |
| *ste6* | SPCC1442.01 | G1-S | Maqbool *et al.*, 2003 | G1 | 140 |
| *srw1* | SPAC144.13c | G1-S | Tournier and Millar, 2000; Yamaguchi *et al.*, 2000 | G1 | 303 |
| *suc22* | SPBC25D12.04 | G1-S | Harris *et al.*, 1996 | G1 | 471 |
| *uvi31* | SPBC16E9.06c | G1 | Kim *et al.*, 1997 | NMD | (1785) |
| *wis3* | SPAC3F10.15c | G2-M | Samuel *et al.*, 2000 | G1 | 43 |

[a] NI, not included in our microarray. NMD, no meaningful data, either because the phases of peak expression were significantly different between the two types of synchronous culture (*) or because the CDC rank (in parentheses) was too low.

peaks of septum-containing cells indicate synchronous septation, which should coincide with the peaks of histone transcript levels and DNA synthesis (Takahashi *et al.*, 2000). Thus, we designated the period around the peak of binucleate cells as M phase and the period around the peak of septum-containing cells as S phase; G1 phase is the period between M and S, and G2 phase is the period between S and M (Figure 1B). The data shown in Figure 1 established that a high degree of synchrony was achieved with both methods.

### *Identification of Cell Cycle-regulated Transcripts*

To identify cell cycle-regulated transcripts, RNA was isolated from synchronous cultures at 10-min intervals and analyzed by microarray hybridization as described in *Materials and Methods*. The data from the two cultures were analyzed separately using an unsupervised algorithm that generated the CDC score (i.e., a quantitative measurement of the degree to which gene expression levels oscillate during the cell cycle) and phase of peak expression for each of 4929 ORFs (see *Materials and Methods*). The final combined CDC scores and phases of peak expression from the two cultures were calculated and used to select the cell cycle-regulated genes (Figure 2A).

Previous studies had identified 43 genes whose transcript levels oscillate in a cell cycle-dependent manner (Table 2). In our study, one of these genes was not included in our microarray, four were filtered out because the cell cycle phase of their peak expression differed significantly between the two types of synchronous cultures, and three were excluded based on low CDC scores (Table 2). Thus, we identified correctly 35 of the 43 previously described cell cycle-regulated transcripts. Accordingly, the false negative rate was no more than ~20% (even if all of the previous reports were accurate). In addition, we estimated a false discovery rate of <1.1% (see *Materials and Methods*). Except in four cases (*mid1*, *rum1*, *sep1*, and *wis3*), the phases of peak expression determined in our study agreed well with those reported previously (Table 2). In addition to the previously known genes, we identified an additional 712 cell cycle-regulated transcripts with similar phase-specific peak expression between the two types of synchronous cultures.

**Table 3.** Cell cycle-regulated genes with characterized functions

| Line | Process | G1 | S | G2 | G2/M | M |
|---|---|---|---|---|---|---|
| 1 | Cell cycle control | *rum1, csk1, mik1* | | *suc1, spd1, wee1, cig1* | *cdc25* | *cdc13, cdr1, nuc2, hcn1* |
| 2 | DNA replication and nucleosome assembly | *cdc18, pfh1, cdc1, cdt1, cdt2, pol1, cdc22, ssb1, suc22, mip1, cdm1* | *hta1, hta2, htb1, hht1, hht2, hht3, hhf1, hhf2, hhf3* | | *cdc23, orc5* | *cdc20, rfc2* |
| 3 | Chromosome organization | *rad21, dfp1, sds21, fin1, smc3, cut2, cnp1* | *sds22* | *hst4, spc24, dhp1, cid14, mis4, cut1* | *cut17* | *cnd1* |
| 4 | Polarized cell growth | *pob1, cdc42, gar2* | *fim1, cam1* | *ppe1, sts5, pho1, pop3, csx2, hob3, pmr1* | *ptc4* | |
| 5 | MT-based processes | *scp3, alp31, klp8* | *nak1* | *dim1, pak1, sad1, alm1, alp14* | *nda2, alp1* | *klp5, tub1, klp6, mph1* |
| 6 | Cytokinesis | *sid2, mob1, imp2, par2, spn2, mid2, cdc4* | | *aps1, rng2, mid1, sep1, myo52* | *myo51, cdc11* | *etd1, cdc15, myp2 plo1, rlc1* |
| 7 | Mating and meiosis | *mfm2, rgs1, spk1, ste6, srw1, byr2, isp6, cig2* | | *sap1, zfs1, mes1, pac2* | | *ste7, mam4, slp1* |
| 8 | RNA pol. subunit | | | *rpb10, rpb3, rpb9* | | |
| 9 | Amino acid biosynthesis | | | *leu2, his3* | | |
| 10 | Protein biogenesis | | *tif34* | *tif51, tif6, tef3, sui1, rps2, rps1202, rpp201, rpp202, rpl901, rpl25a, rpl3202, rps13, rpl2701, rpl29, rpl3801* | *rpl1603* | |
| 11 | Transport/secretion | *bet1, emp24, erv14, sec22, anc1* | *rer1, sod2, clc1, fio1, ght3, ypt3, sec17* | *arf1, n150, kap104, ght2, bfr1, nup124, nrf1, pmd1, mae1, pim1, apl1, pse1, sec72, sar1* | *sec1* | *sly1, abc1, sso1* |
| 12 | Lipid/sterol metabolism | | *erg7, cut6* | *erg28, lsd1, ipk1* | | *bem46, gpi1* |
| 13 | Cell wall biogenesis | *chs2, exg1, eng1, pmk1, bgs4* | | *cwl1, psu1, gmh2, bgs3, hsf1, atf1, gpx1, ctt1, sks2, mpr1, hsp9, wis4, wis1, csx1, sin1, hsp60, bip1* | *exg2* | *cwg2, ags1* |
| 14 | Stress response | | | | *slm9* | |
| 15 | Carbohydrate metabolism | *fum1* | | *scr1* | | |
| 16 | Ubiquitin modification | *ubc15, ubc3* | *pub1* | *ubi4, ubi3, ubi1* | | *ubc11* |
| 17 | DNA repair | *msh6* | | *rad25, rdp1, top2, hus2* | *ung1* | *pms1, pac1, mus81* |

[a] More information and relevant references on these genes can be obtained through the websites of the Sanger Centre GeneDB (http://www.genedb.org) and Incyte PombeDB (http://www.incyte.com/proteome).

The complete list of 747 cell cycle-regulated genes ordered on the basis of phase of peak expression is available at http://giscompute.gis.a-star.edu.sg/~gisljh/CDC.

### *Characterization of Known Transcripts by Cell Cycle Phases*

Of the 747 cell cycle-regulated genes, >200 have been characterized functionally (and thus assigned gene symbols) based on the pombeDB (Incyte, Beverly, MA) and/or gene DB (Sanger Institute, Hinxton, United Kingdom) (Table 3). Many of these genes showed peaks in transcript abundance that correlated well with the times at which their products are thought to function during the cell cycle. For example, ≥11 genes whose products are implicated in cell cycle control had cell cycle-regulated transcripts (Table 3, line 1). Among these, *wee1* and *cdc25* showed peaks in G2 and G2/M, respectively, consistent with the role of Wee1p in negatively regulating Cdc2p during interphase and the role of Cdc25p in activating Cdc2p during the entry into mitosis (Russell and Nurse, 1986). In addition, many genes whose products function in DNA replication, nucleosome assembly, or chromosome organization had peaks of expression in G1 or S (Table 3, lines 2 and 3); several genes whose products function in the polarization of cell growth had peaks of expression in G1, S, or G2 (the phases in which polarized growth is established and carried out) (Table 3, line 4); several genes whose products probably function in the mitotic spindle had peaks of expression in G2/M or M (Table 3, line 5); and many genes whose products function in cytokinesis and/or septation had peaks of expression in M or G1 (which overlaps with the time of septum formation in *S. pombe*) (Table 3, line 6). Interestingly, many genes whose products function in sexual development also had peaks of expression in M or G1 (Table 3, line 7), consistent with the evidence that sexual development can only initiate from the G1 phase (Borgne *et al*., 2002).

G2 occupies ~70% of the cell cycle in rapidly growing *S. pombe* cells, and it is accordingly when most increase in cell mass occurs (MacNeill and Nurse, 1997). Thus, it was not surprising to find that many genes whose products are involved in aspects of biosynthesis (transcription, amino acid and protein biosynthesis, protein transport and secretion, lipid metabolism, and cell wall biogenesis) had peaks of expression in G2 (Table 3, lines 8–13). Perhaps more surprising was the finding that many stress response genes had peaks of expression in G2 (Table 3, line 14). This may reflect a need to respond continually to stresses that arise as the plasma membrane and cell wall are remodeled as the cell grows during G2.

### *Cluster Analysis of Cell Cycle-regulated Genes*

Many of the genes known previously to display cell cycle-regulated transcription have expression peaks around the G1-S or M-G1 interval and are thought to be regulated by the transcription factor complexes DSC (G1/S) and PBF (M/G1) (see Introduction). In addition, the S phase-specific transcription of the histone genes is thought to depend on the regulatory sequence ATCAMAACCCTAACCCT in their promoter regions (Choe *et al*., 1985; Matsumoto and Yanagida, 1985), although the transcription factors involved have not been identified. To identify additional members of these and other coregulated sets of genes, we analyzed the complete set of 747 genes by hierarchical clustering of transcripts with similar expression patterns. We used an uncentered Pearson correlation matrix with complete linkage (Eisen *et al*., 1998) (Figure 2B). As expected, we found a cluster of ~31 genes that were expressed predominantly in G1 and were strongly associated ($p$ value $<2.7 \times 10^{-7}$) with the MCB (DSC-controlled) promoter motif. In addition, three other promoter motifs were found to have strong associations with sets of cell cycle-regulated genes (Figure 2A). One cluster of G1- and S-phase genes was found to contain the ACE2 motif ($p$ value $<3.5 \times 10^{-4}$); one cluster of G2-phase genes contains the ATF motif ($p$ value $<1.6 \times 10^{-8}$); and two clusters of M- and G1-phase genes were found to contain SFF motifs ($p$ value $<1.0 \times 10^{-8}$) (Figure 2B). We also identified several clusters enriched for genes that have common biological functions but lack known common promoter elements. Two such clusters contain largely G2-expressed genes encoding ribosomal proteins (RiP) (Figure 2B). Each of these clusters is discussed in more detail below. Surprisingly, we did not find a cluster of genes to be strongly associated with the PCB (PBF-controlled) promoter motif (Figure 2A; see, however, below).

### *G1-Phase Clusters*

As noted above, we found an "MCB cluster" of ~31 G1-expressed genes of which most (19) possessed one or more MCB motifs within 1 kb of the start codon (Figure 3A). A 20th gene, *cig2*, has MCB motifs that are >1 kb from its start codon but are still functional in controlling its expression (Ayte *et al*., 2001; see below). To ask whether expression of these genes is regulated by the DSC complex, we used mutations affecting Cdc10p, a component of the complex. Cells harboring the gain-of-function mutant allele *cdc10-C4* allele have been shown to accumulate several MCB-motif-containing transcripts at permissive temperature (McInerny *et al*., 1995). Similarly, we found that 15 of the 20 genes with MCB motifs showed noticeable transcript accumulation relative to wild-type in at least two of three independent cultures (Figure 3A). We further tested DSC dependency by using the temperature-sensitive loss-of-function allele *cdc10-V50* (Reymond *et al*., 1992; Rowley *et al*., 1992; see *Materials and Methods*). Analysis of mitotic and septation indices and of DNA contents confirmed that G1 arrest occurred as expected (Figure 3B, top). Fifteen of the 20 MCB motif-containing genes showed reduced expression in the *cdc10-V50* culture, indicating DSC-dependent expression (Figure 3B, bottom). All of these genes contained two or more MCB motifs, and 14 of them also had been indicated to be DSC dependent by the *cdc10-C4* experiment. Thus, only two of the MCB motif-containing genes, SPBC1709.12 and SPBC1442.01/*ste6*, gave inconsistent results in the two tests of DSC dependency. The reason for this discrepancy is not known, although we note that *ste6* contains only one MCB motif. The genes identified here as DSC-dependent include some (*cdc18*, *cdc22*, *cdt1*, *cig2*, and *mik1*) that were previously known to be so and others that were not. Together, the data suggest that regulation of genes required for the G1/S transition or for DNA synthesis depends on double or multiple MCB motifs.

In contrast, among the 11 genes that were originally identified as members of the MCB cluster but have no detectable MCB motifs, none seemed to be DSC dependent by both of the tests described above. In investigating further the regulation of these genes, we noted that many members of the MCB gene cluster (and 6 of the 11 seemingly DSB-independent genes) contained ACE2 motifs in their promoters, suggesting that transcription factors that use these motifs may regulate their G1-specific expression. In support of this hypothesis, we also found an ACE2 cluster of genes very close to the MCB cluster in the dendrogram of Figure 2B, as noted above. The genes in this cluster seemed to be DSC independent by both the *cdc10-V50* and *cdc10-C4* tests (our unpublished data). In contrast, profiling of a mutant lacking the putative transcription factor Ace2p (Martin-Cuadrado *et al*., 2003) indicated reduced expression of these genes, suggesting a cell cycle-specific transcription activity for Ace2p (Figure 3C). Most of the previously characterized genes in the ACE2 cluster encode proteins involved in cytokinesis and septation (such as Cdc4p, Bgs4p, and Mid2p). Together, the data suggest that there are at least two transcriptional machineries regulating gene expression around the G1 phase: one specific for the G1/S transition and DNA replication that uses MCB motifs and another specific for cytokinesis and septation that uses ACE2 motifs.

### *S- and G2-Phase Clusters*

Large quantities of new histone proteins are required to form functional chromatin during S phase. Accordingly, transcription of histone genes has been found to be S phase specific in both *S. pombe* (Choe *et al*., 1985; Matsumoto *et al*., 1985) and a variety of other organisms. We found that eight of the nine *S. pombe* histone genes formed a very prominent S phase cluster (Figures 2B and 4A and Tables 2 and 3). One of the three histone H3 genes (*hht2*) was missing from the cluster, and only one other gene (*sds22*, encoding a subunit of protein phosphatase PP1) seemed to be coregulated.

As noted above, the importance of growth during the G2 phase is correlated with the G2-specific expression of many growth-associated genes such as ribosomal protein genes. This was reflected in the cluster analysis by the appearance of two clusters containing many of these genes, the RiP clusters (Figures 2B and 4, B and C). Interestingly, however, only 10 of the ~130 ribosomal protein genes were found in our set of 747 cell cycle-regulated genes; eight of these were in one of the RiP clusters.

As noted above, another G2-phase gene cluster (Table 3, line 14, and Figures 2B and 4D) showed a strong association with ATF promoter motifs, which are targets of ATF/CREB-like

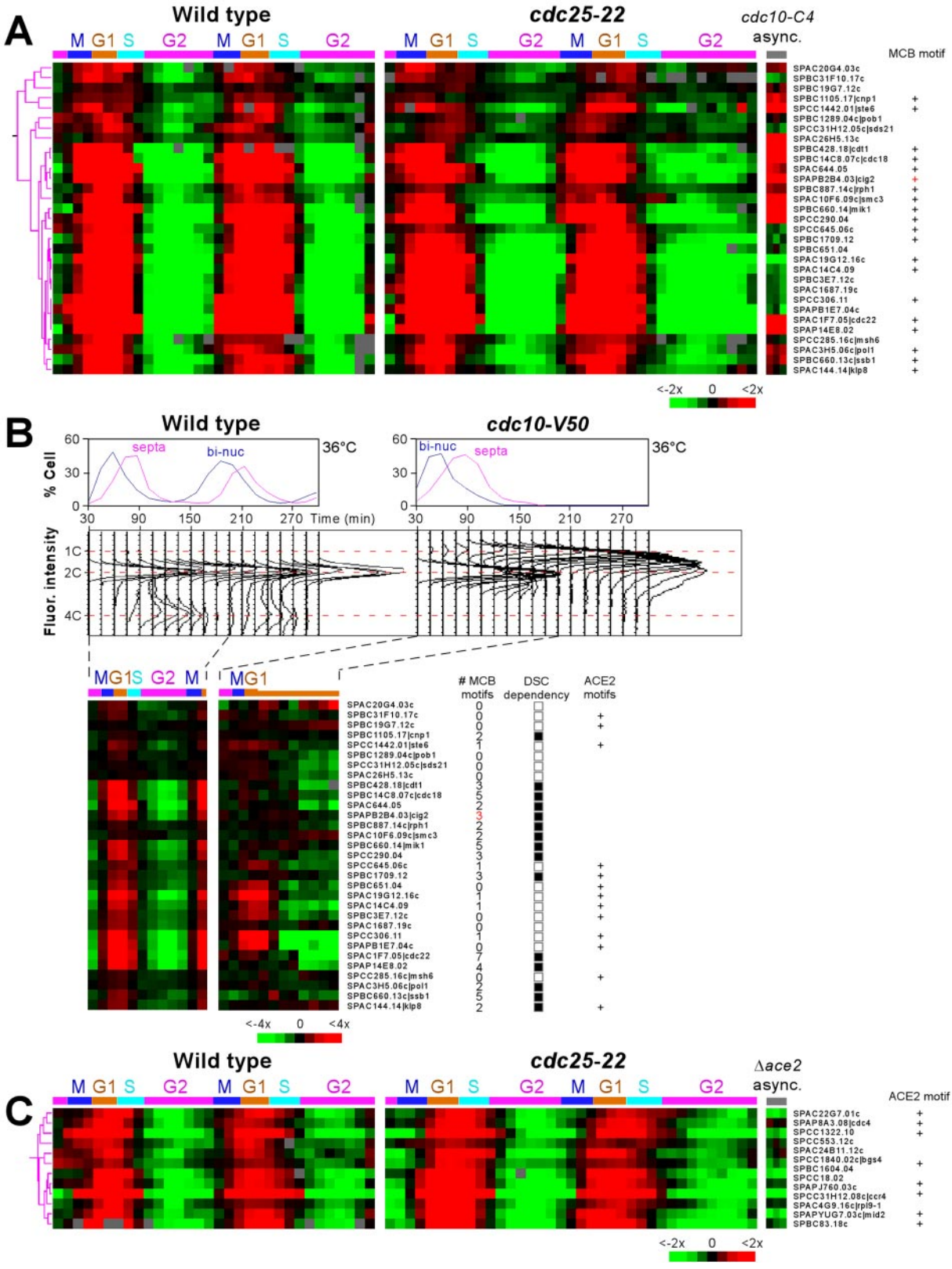


**Figure 3.** The G1-phase clusters. The transcription profiles are displayed as in Figure 2B. The systematic names plus the gene symbols (where available) are listed on the right. Genes possessing the indicated promoter motifs are marked by a "+" on the right. (A) Expanded view of the MCB cluster (see Figure 2B). The red + indicates that the MCB motifs are not within 1 kb of the start codon (see text). The expression profiles from three independent asynchronous cultures of the *cdc10-C4* mutant at permissive temperature (vs. asynchronous wild-type cells as reference) are also shown. (B) Perturbation of the DSC transcriptional activity by use of a *cdc10* mutation (see *Materials and Methods*). The top two panels show mitotic index (binuc), septation index (septa), and DNA contents of the elutriation-synchronized wild-type

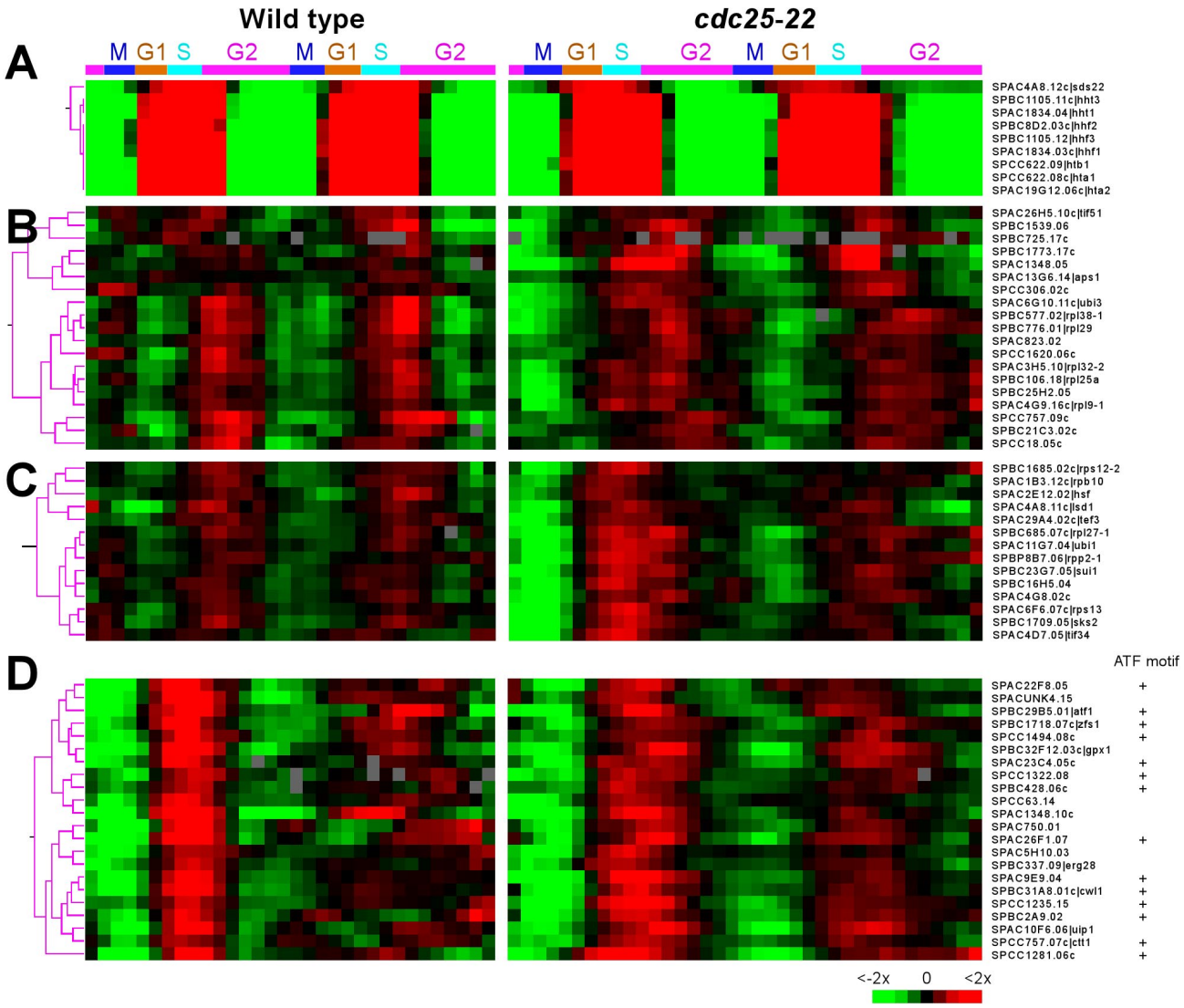


**Figure 4.** The S- and G2-phase clusters. The transcription profiles and gene symbols are displayed as in Figures 2B and 3. (A) The S-phase cluster. (B and C) The two RiP clusters containing ribosomal protein genes. (D) The ATF cluster. The presence or absence of ATF motifs is indicated on the right.

transcriptional factors during cellular response to environmental stresses in *S. cerevisiae* (Sellers *et al.*, 1990). Because several of the genes in this cluster are known to be involved in stress response pathways in *S. pombe*, they are probably also regulated by transcription factors similar to ATF/CREB.

### *M-Phase Clusters*

We found two clusters of M- or M/G1-phase genes that were strongly associated with SFF promoter motifs (Figures 2B and 5). SFF (SWI5 factor) motifs (Lydall *et al.*, 1991), together with MCM1 motifs, have previously been shown to regulate M-phase genes in *S. cerevisiae* (Spellman *et al.*, 1998). However, we did not find an association with MCM1 motifs, suggesting that this regulatory role is restricted to SFF motifs in *S. pombe*. Interestingly, many genes that previously were shown to contain PCB motifs and to be regulated by the PBF transcription factors (Anderson *et al.*, 2002) were found in our study to be members of the SFF clusters. Although the PCB motif did not seem to be associated with cell cycle-regulated genes in our analysis (Figure 2A), the PCB sequence G*MAAC*R is very similar to the SFF motif GT*MAAC*AA, suggesting that the SFF motif could be a variant of the PCB motif and thus used by PBF transcription factors. The forkhead domain-containing transcription factor Sep1p has been shown to regulate transcription of *cdc15*, one of the SFF cluster genes (Zilahi *et al.*, 2000). We therefore investigated whether other genes in the cluster were regulated by Sep1p. In support of this hypothesis, many SFF-motif-

**Figure 3 (cont).** and *cdc10-V50* mutant cultures at 36°C. The bottom panel shows the expression profiles of the MCB cluster genes. The solid boxes on the right indicate genes whose G1 expression was reduced in the *cdc10* mutant and thus are classified as DSC dependent. The numbers of MCB and ACE2 motifs associated with each gene are also indicated. (C) Expanded view of the ACE2 cluster (see Figure 2B). The expression profiles from three independent asynchronous cultures of the Δ*ace2* mutant (vs. asynchronous wild-type cells as reference) also are shown.

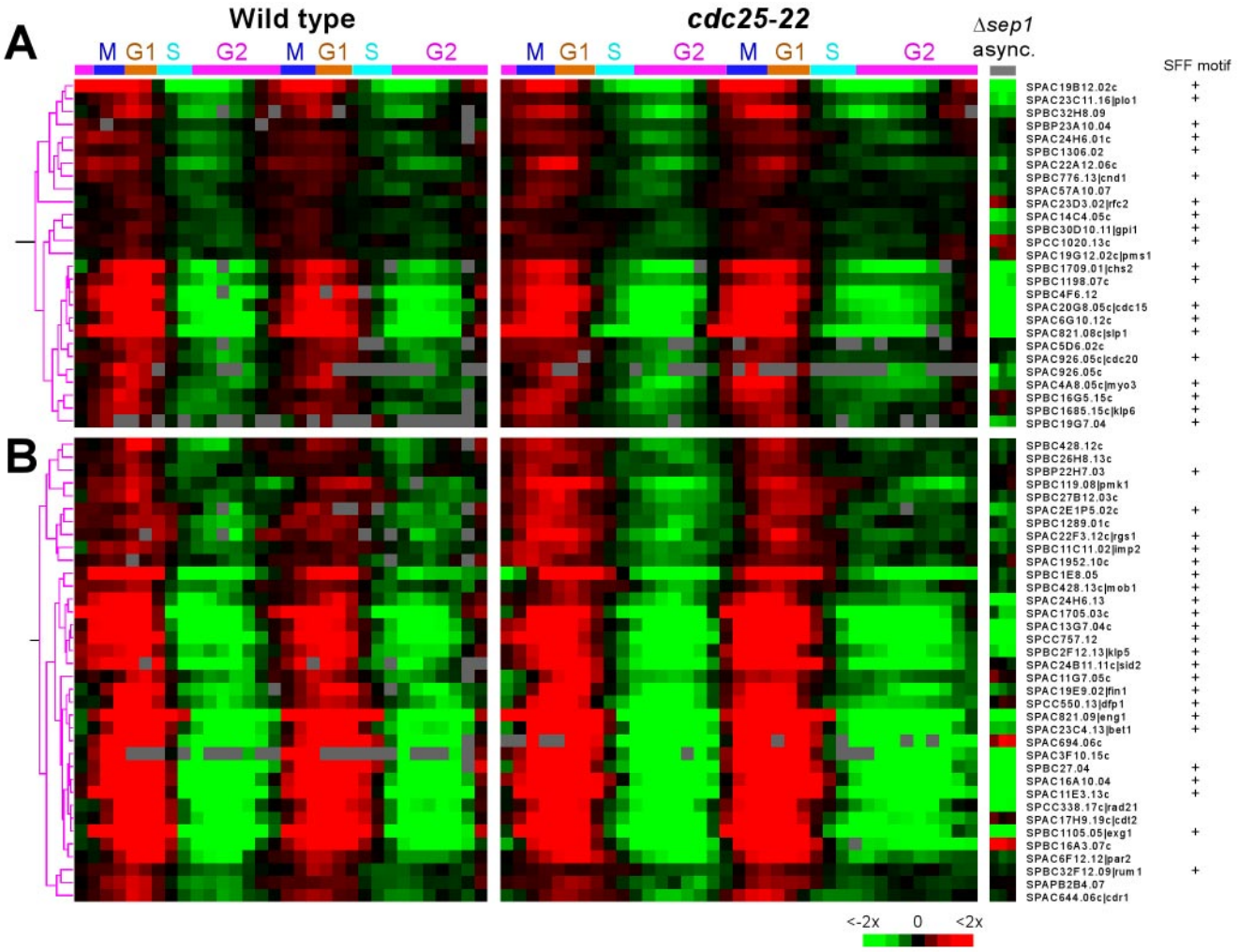


**Figure 5.** The M-phase clusters. The transcription profiles and gene symbols are displayed as in Figures 2B and 3. The presence or absence of SFF motifs is indicated on the right. The expression profiles from three independent asynchronous Δ*sep1* mutant cultures (vs. asynchronous wild-type cells as reference) also are shown. (A) The SFF (1) cluster. Most genes have peak expression in M phase. (B) The SFF (2) cluster. Most genes have peak expression in either M or G1 phase.

containing genes were indeed down-regulated in a Δ*sep1* mutant (Figure 5, A and B).

### *Search for Cell Cycle-specific Promoter Motifs*

To search for other promoter motifs that might regulate cell cycle-specific expression, we analyzed the distributions in the promoter regions of the 747 cell cycle-regulated genes of motif sequences that have been characterized previously in *S. cerevisiae* (see *Materials and Methods*). However, among ~50 different motifs that we tested, only the four motifs described above (SFF, MCB, ACE2, and ATF) were found to exhibit statistically significant differential distributions among the 747 genes (Figure 2A). Although PCB motifs have been associated previously with several genes with peak transcription at M-G1 (Anderson *et al*., 2002), we found no such association, apparently because of the abundance of such motifs, which are present in 458 of the 747 cell cycle-regulated genes (see *Materials and Methods*). Thus, it seems unlikely that the PCB motif plays an important role in mediating cell cycle-specific gene expression.

### *Comparison of Cell Cycle-regulated Genes between Fission and Budding Yeast*

*S. pombe* and *S. cerevisiae* are thought to have diverged evolutionarily ~$10^9$ yr ago (Heckman *et al*., 2001). Although the two yeasts share many cell cycle regulators, their cell cycles also show some differences in organization. For example, during rapid growth, *S. pombe* cells have a long G2 phase during which most growth occurs, and the major cell cycle checkpoint is at the G2/M transition. In contrast, *S. cerevisiae* daughter cells typically have an extended G1 phase during which growth to a critical size is achieved, and the major cell cycle checkpoint in both daughter and mother cells is at the G1/S transition. We therefore hypothesized the existence of two classes of cell cycle genes: those that are directly involved in cell cycle progression and those that are not (e.g., genes controlling metabolism and cell growth) but whose expression must be coordinated with certain cell cycle phases. To test this hypothesis, we compared the set of cell cycle-regulated genes identified here to those identified in *S. cerevisiae* (Spellman *et al*., 1998) by using a similar experimental approach. Using a current table of *S. pombe* and

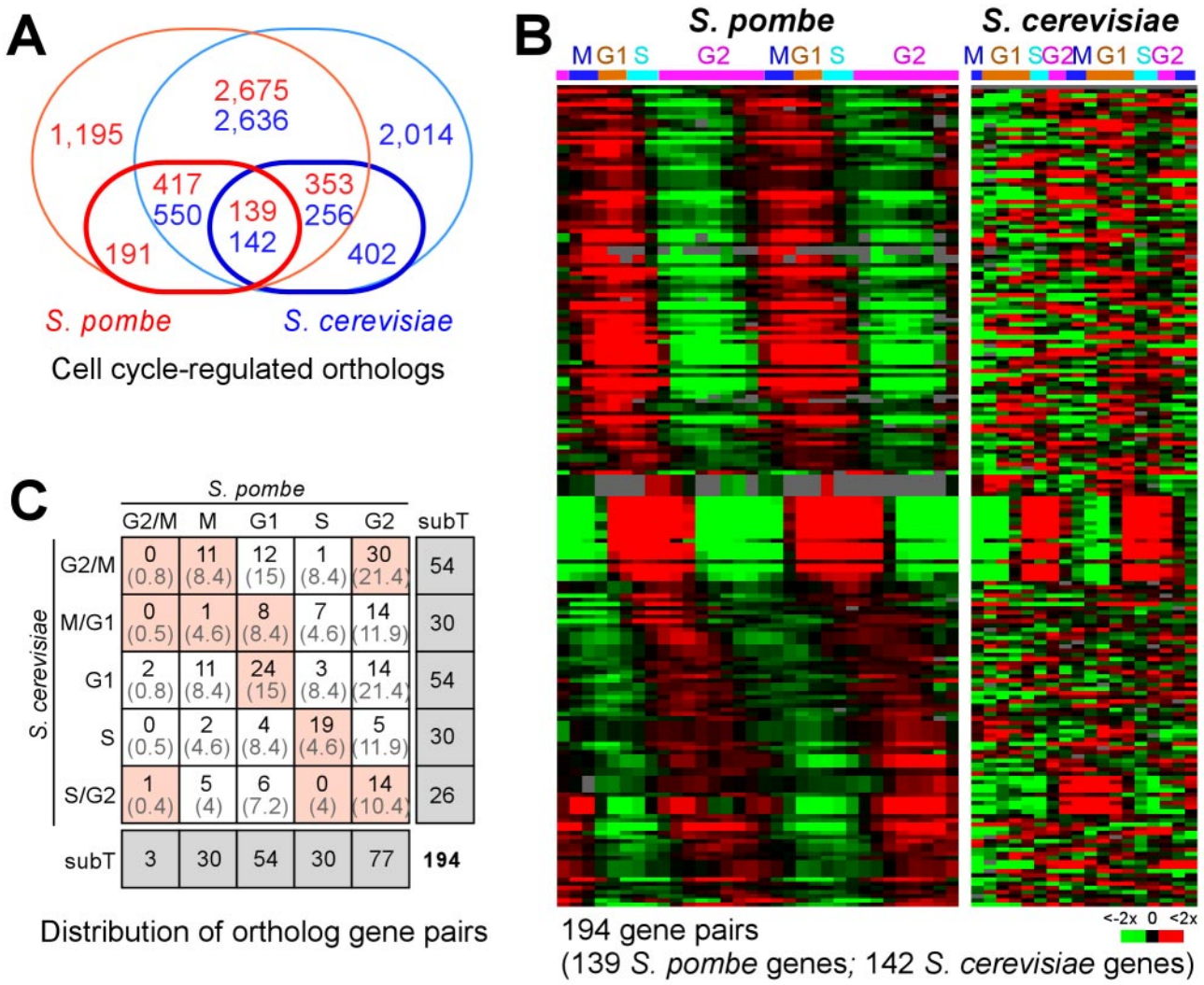


**Figure 6.** *S. pombe* and *S. cerevisiae* orthologues showing cell cycle-regulated expression. (A) Venn diagram summarizing orthologies and cell cycle-regulated expression in the two yeasts. The thin red (blue) circle and the sum of red (blue) numbers represent the 4970 (6000) ORFs in *S. pombe* (*S. cerevisiae*). The thick circles and enclosed numbers represent the cell cycle-regulated genes. Thus, 139 *S. pombe* genes with 142 *S. cerevisiae* orthologues (including multiple-gene pairs, or co-orthologs) were cell cycle regulated in both yeasts; 417 *S. pombe* genes with 550 *S. cerevisiae* orthologues were cell cycle regulated in *S. pombe* but not in *S. cerevisiae*; and so on. (B) Expression profiles of the ~140 orthologues as separated into 194 one-to-one pairs (see text). Expression profiles of the 139 *S. pombe* genes were displayed based on the elutriation experiment and ordered based on the timing of their peak expression (cf. Figure 2A). Expression profiles of the 142 *S. cerevisiae* genes were based on the α-factor experiment (Spellman *et al.*, 1998) and ordered according to their orthologues in *S. pombe*. (C) Distribution of the peak-expression phases for the 194 ortholog pairs. The numbers of gene pairs in each category are based on the assignment of peak-expression phases for the individual genes in *S. pombe* (this study) and *S. cerevisiae* (Spellman *et al.*, 1998). Numbers in parentheses are the expected numbers of pairs based on the subtotals for each yeast (gray-shaded boxes) and the assumption of no correlation in peak-expression phases between the two yeasts. Pink-shaded and unshaded boxes indicate gene pairs with concordant and discordant expressions, respectively.

*S. cerevisiae* orthologues (Wood, personal communication), we found that 139 of the 747 cell cycle-regulated genes identified in *S. pombe* have 142 orthologues among the 800 cell cycle-regulated genes found in *S. cerevisiae* (Figure 6A). Of the ~140 cell cycle-regulated genes common to both species, many (~50) encode proteins involved in cell cycle-specific processes such as DNA replication, chromosome maintenance, and cell cycle control and may represent the core of transcriptionally regulated, cell cycle-specific genes that have been conserved over a large evolutionary distance.

To compare the orthologue expression patterns between the two yeasts, we first generated a list of 194 one-to-one orthologue pairs between the 139 genes in *S. pombe* and the 142 genes in *S. cerevisiae*. Then, we compared the expression profiles of these gene pairs by using a phasogram format that should allow a systematic view of similarities in expression patterns (Figure 6B). Interestingly, such similarities were not readily apparent, suggesting that there are marked differences between orthologues in their phases of peak expression. Therefore, we grouped the orthologue pairs according to their assigned phases of peak expressions (Figure 6C), which revealed that the distribution of pairs with concordant phasing of peak expression was highly significant ($p < 2 \times 10^{-12}$) by the $\chi^2$ test. Thus, we then separated orthologue pairs that displayed concordant phasing of peak expression from those with discordant phasing. Of the 108

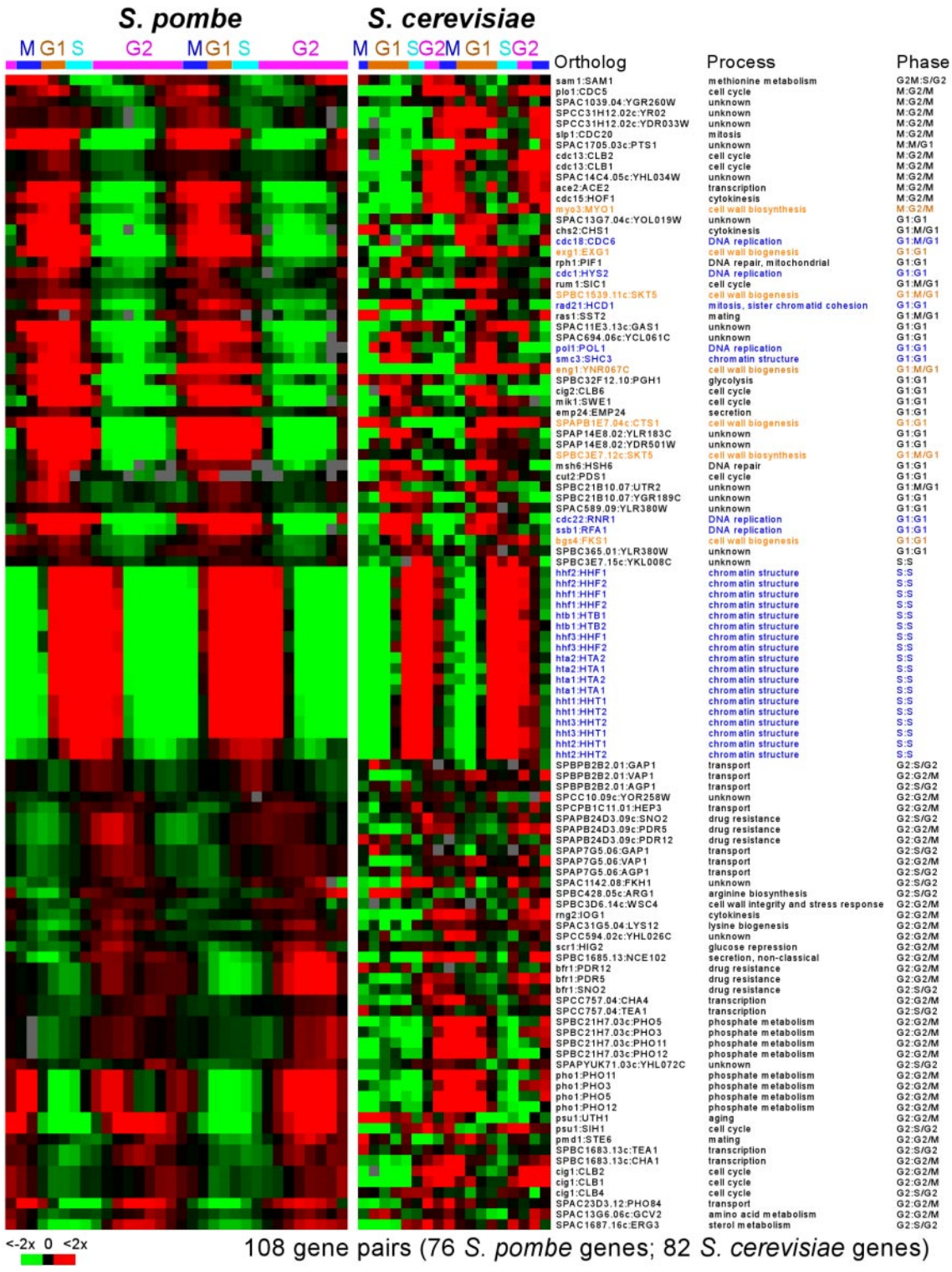


**Figure 7.** Expression profiles of the 108 orthologue pairs with concordant phases of peak expression. The transcription profiles are displayed as in Figure 6B. The assigned phases of peak expression and functions in biological processes (where known) of the gene pairs are given. Genes encoding proteins involved in DNA replication or chromosome structure are shown in blue; genes encoding proteins involved in cell wall biogenesis or cytokinesis are shown in brown.

pairs with concordant phasing ≥25 were found to encode proteins involved in DNA replication or chromosome structure, as highlighted in blue in Figure 7.

Comparative analysis of the expression patterns of the orthologue pairs with discordant phases of peak expression revealed that some of these genes encode proteins involved


**Figure 8.** Expression profiles of the 86 orthologues with discordant phases of peak expression. Information is displayed as described in Figure 7.

in cell metabolism and growth or in cell wall biogenesis (Figure 8). For example, *S. pombe exg2* and SPAC19B12.02c were up-regulated at the end of G2 and down-regulated at the end of G1, whereas the *S. cerevisiae* orthologues *EXG2* and *GAS1* had nearly the opposite pattern. Such findings might reflect the differing roles of G1 and G2 in the two yeasts as noted above. Interestingly, however, several orthologue pairs thought to be involved in cell wall biogenesis also were found to exhibit concordant expression patterns, with peak expression in G1 (Figure 7). This may reflect specific functions for such proteins in G1 in both yeasts, such as the assembly of the division septum at cytokinesis.

## DISCUSSION

We have identified 747 *S. pombe* genes whose expression levels oscillate during the cell cycle both in wild-type cultures synchronized by elutriation and in *cdc25* mutant cultures synchronized by block-and-release. Of 43 genes shown previously to have cell cycle-regulated expression, 35 also were identified in our study, suggesting a false negative rate of ≤20%. Most of these genes displayed high dynamic expression ranges of greater than threefold compared with those of asynchronous references. We also estimated a low false discovery rate of ~1%. Together, the data suggest that

our approach is of high sensitivity and accuracy (cf. Spellman *et al*., 1998; Whitfield *et al*., 2002).

Of the 747 genes, ~200 were previously known to be involved in cell cycle-specific processes such as DNA replication, chromosome structure and maintenance, cell wall biogenesis, cytokinesis, and cell cycle control. Cluster analyses of expression patterns identified groups containing both known genes and uncharacterized ORFs, which permits assigning possible functions to these ORFs based on those of the known genes in the same groups. In addition, perturbing the activities of the DSC, Ace2p, and Sep1p transcription factors revealed subsets of functional targets and helped to define the corresponding promoter requirements. Together, our results are consistent with the hypothesis that cell cycle-regulated genes play an important role in cell cycle progression (Spellman *et al*., 1998; Futcher, 2000; Whitfield *et al*., 2002; Maqbool *et al*., 2003).

Promoter-motif analysis revealed four motifs (of ~50 different motifs tested) that were found preferentially associated with sets of cell cycle-regulated genes. These motifs were associated with expression at different phases: M-G1 (the SFF motifs that may be used by the putative transcription factor Sep1p); G1 (the MCB motifs used by the DSC transcription factor); G1-S (the ACE2 motifs that may be used by the putative transcription factor Ace2p); and G2 (the ATF motifs). Interestingly, each of these motifs, except for ATF, has been shown to be involved in the cell cycle transcriptional circuitry in *S. cerevisiae* (Spellman *et al*., 1998; Simon *et al*., 2001). However, experimental tests of the roles of the SFF, ACE2, and ATF motifs in regulation of cell cycle-specific expression in *S. pombe* have yet to be performed.

Based on a table of genes orthologous between *S. pombe* and *S. cerevisiae* and the data of Spellman *et al*. (1998) on the expression of *S. cerevisiae* genes, we found ~140 genes whose orthologues in both yeasts exhibit cell cycle-regulated expression. Comparative analysis of these ~140 genes revealed a subset of highly conserved genes that display concordant phases of peak expression; many of these genes encode proteins directly involved in aspects of the nuclear division cycle such as DNA replication and chromosome structure maintenance. In contrast, at least some orthologue pairs that did not display similar phases of peak expression seem to play roles in cell cycle-accompanying processes such as growth and aspects of cell wall biogenesis whose timing may be organism specific.

During the revision of our article, a similar study was reported by Rustici *et al*. (2004), in which the authors identified 407 cell cycle-regulated genes. By using a Fast Fourier Transformation algorithm, these investigators first generated a list of ~1000 genes that met the criteria for cell cycle-modulated expression. This list was further trimmed to 407 genes by the use of additional criteria such as the removal of genes whose oscillation ranges were <1.5-fold (160 of 407, or 39%, had ranges >2-fold). In this study, we have uncovered 747 cell cycle-regulated genes, of which 313 (42%) displayed dynamic ranges of ≥2-fold, 387 (52%) had ranges of 1.5- to 2-fold, and 47 (6%) had ranges of 1.32- to 1.5-fold. About 60% (242) of the cell cycle-regulated genes found by Rustici *et al*. (2004) are also in our list of 747 genes (see Supplemental Table 1). Of these 242 genes, 207 were in the top 500 of our 747 genes based on our CDC scores and thus had relatively high dynamic oscillation ranges in our study. Thus, good matches of the two data sets were found for genes exhibiting high dynamic oscillation ranges, suggesting that the differences between the two data sets can probably be attributed to different sensitivities in detecting transcript levels. Our study used oligonucleotide-based microarray technology to analyze 36 time-points that covered two cell cycles (~6 h at 10-min intervals), whereas Rustici *et al*. (2004) used cDNA microarray technology to analyze 24 time-points that also covered two cell cycles (~6 h at 15-min intervals). It has been shown that the oligo-based microarray technology is more sensitive than the cDNA technology in detecting ORF-specific expression (Carter *et al*., 2003). In addition our higher sampling rate could have significantly increased the sensitivity of the algorithms for detecting transcripts whose levels oscillate.

We hope that our results will be useful for the further analysis of the genes with distinctive expression patterns and for comparisons with similar data from other systems. A complete data set from this study is available at http://giscompute.gis.a-star.edu.sg/~gisljh/CDC.

## ACKNOWLEDGMENTS

We thank Y. Kun and K. Gong for assistance in spotting microarrays, Y. Kuang for maintenance and update of databases, and Dr. P. Long for valuable comments on the algorithm for detecting cell cycle-regulated transcripts. We are indebted to Dr. V. Wood for providing the table of fission and budding yeast orthologues before publication. We thank Drs. C. J. McInerny and M. Sipiczki for strains and Drs. T. Lufkin, P. Robson, J. George, S. Gupta, and V. M. D'Souza for discussion and critical reading of the manuscript. We appreciate comments by the monitoring editor Dr. J. R. Pringle and three anonymous reviewers that significantly improved the manuscript. This work was supported by Temasek Life Sciences Laboratory, Singapore, the Agency for Science, Technology and Research, Singapore (A-STAR), and a Genome Institute of Singapore/A-STAR grant (#GIS/03-113401) to J. L.

## REFERENCES

Alemany, V., Sanchez-Piris, M., Bachs, O., and Aligue, R. (2002). Cmk2, a novel serine/threonine kinase in fission yeast. FEBS Lett. *524*, 79–86.

Anderson, M., Ng, S. S., Marchesi, V., MacIver, F. H., Stevens, F. E., Riddell, T., Glover, D. M., Hagan, I. M., and McInerny, C. J. (2002). plo1$^{+}$regulates gene transcription at the M-G$_1$interval during the fission yeast mitotic cell cycle. EMBO J. *21*, 5745–5755.

Ayte, J., Schweitzer, C., Zarzov, P., Nurse, P., and DeCaprio, J. A. (2001). Feedback regulation of the MBF transcription factor by cyclin Cig2. Nat. Cell Biol. *3*, 1043–1050.

Bähler, J., Wu, J.-Q., Longtine, M. S., Shah, N. G., McKenzie, A., Steever, A. B., Wach, A., Philippsen, P., and Pringle, J. R. (1998). Heterologous modules for efficient and versatile PCR-based gene targeting in *Schizosaccharomyces pombe*. Yeast *14*, 943–951.

Benito, J., Martín-Castellanos, C., and Moreno, S. (1998). Regulation of the G1 phase of the cell cycle by periodic stabilization and degradation of the p25$^{rum1}$CDK inhibitor. EMBO J. *17*, 482–497.

Birkenbihl, R. P., and Subramani, S. (1995). The *rad21*gene product of *Schizosaccharomyces pombe* is a nuclear, cell cycle-regulated phosphoprotein. J. Biol. Chem. *270*, 7703–7711.

Borgne, A., Murakami, H., Ayte, J., and Nurse, P. (2002). The G1/S cyclin Cig2p during meiosis in fission yeast. Mol. Biol. Cell *13*, 2080–2090.

Brown, G. W., and Kelly, T. J. (1999). Cell cycle regulation of Dfp1, an activator of the Hsk1 protein kinase. Proc. Natl. Acad. Sci. USA *96*, 8443–8448.

Caligiuri, M., and Beach, D. (1993). Sct1 functions in partnership with Cdc10 in a transcription complex that activates cell cycle START and inhibits differentiation. Cell *72*, 607–619.

Carr, A. M., Dorrington, S. M., Hindley, J., Phear, G. A., Aves, S. J., and Nurse, P. (1994). Analysis of a histone H2A variant from fission yeast: evidence for a role in chromosome stability. Mol. Gen. Genet. *245*, 628–635.

Carter, M. G., *et al*. (2003). In situ-synthesized novel microarray optimized for mouse stem cell and early developmental expression profiling. Genome Res. *13*, 1011–1021.

Chen, E. S., Saitoh, S., Yanagida, M., and Takahashi, K. (2003). A cell cycle-regulated GATA factor promotes centromeric localization of CENP-A in fission yeast. Mol. Cell. *11*, 175–187.

Cho, R. J., *et al*.(1998). A genome-wide transcriptional analysis of the mitotic cell cycle. Mol. Cell. *2*, 65–73.

Cho, R. J., Huang, M., Campbell, M. J., Dong, H., Steinmetz, L., Sapinoso, L., Hampton, G., Elledge, S. J., Davis, R. W., and Lockhart, D. J. (2001). Transcriptional regulation and function during the human cell cycle. Nat. Genet. *27*, 48–54.

Choe, J., Schuster, T., and Grunstein, M. (1985). Organization, primary structure, and evolution of histone H2A and H2B genes of the fission yeast *Schizosaccharomyces pombe*. Mol. Cell. Biol. *5*, 3261–3269.

Christensen, P. U., Bentley, N. J., Martinho, R. G., Nielsen, O., and Carr, A. M. (2000). Mik1 levels accumulate in S phase and may mediate an intrinsic link between S phase and mitosis. Proc. Natl. Acad. Sci. USA *97*, 2579–2584.

Ducommun, B., Draetta, G., Young, P., and Beach, D. (1990). Fission yeast *cdc25*is a cell-cycle regulated protein. Biochem. Biophys. Res. Commun. *167*, 301–309.

Eisen, M. B., Spellman, P. T., Brown, P. O., and Botstein, D. (1998). Cluster analysis and display of genome-wide expression patterns. Proc. Natl. Acad. Sci. USA *95*, 14863–14868.

Fankhauser, C., Reymond, A., Cerutti, L., Utzig, S., Hofmann, K., and Simanis, V. (1995). The *S. pombe cdc15*gene is a key element in the reorganization of F-actin at mitosis. Cell *82*, 435–444.

Forsburg, S. L., and Nurse, P. (1994). The fission yeast *cdc19*$^+$gene encodes a member of the MCM family of replication proteins. J. Cell Sci. *107*, 2779–2788.

Futcher, B. (2000). Microarrays and cell cycle transcription in yeast. Curr. Opin. Cell Biol. *12*, 710–715.

Hagan, I. M., and Hyams, J. S. (1988). The use of cell division cycle mutants to investigate the control of microtubule distribution in the fission yeast *Schizosaccharomyces pombe*. J. Cell Sci. *89*, 343–357.

Harris, P., Kersey, P. J., McInerny, C. J., and Fantes, P. A. (1996). Cell cycle, DNA damage and heat shock regulate *suc22*$^+$expression in fission yeast. Mol. Gen. Genet. *252*, 284–291.

Heckman, D. S., Geiser, D. M., Eidell, B. R., Stauffer, R. L., Kardos, N. L., and Hedges, S. B. (2001). Molecular evidence for the early colonization of land by fungi and plants. Science *293*, 1129–1133.

Hofmann, J.F.X., and Beach, D. (1994). cdt1 is an essential target of the Cdc10/Sct1 transcription factor: requirement for DNA replication and inhibition of mitosis. EMBO J. *13*, 425–434.

Kane, M. D., Jatkoe, T. A., Stumpf, C. R., Lu, J., Thomas, J. D., and Madore, S. J. (2000). Assessment of the sensitivity and specificity of oligonucleotide (50mer) microarrays. Nucleic Acids Res. *28*, 4552–4557.

Karuturi, K. M., and Liu, J. (2004). Improved Fourier Transform method for unsupervised cell-cycle regulated gene prediction. In: Proceedings of the 2004 IEEE Computational Systems Bioinformatics Conference, Stanford, CA (http://conferences.computer.org/bioinformatics/CSB2004/Program4.htm).

Kelly, T. J., Martin, G. S., Forsburg, S. L., Stephen, R. J., Russo, A., and Nurse, P. (1993). The fission yeast *cdc18*$^+$gene product couples S phase to START and mitosis. Cell *74*, 371–382.

Kim, S.-H., Kim, M., Lee, J. K., Kim, M. J., Jin, Y. H., Seong, R. H., Hong, S. H., Joe, C. O., and Park, S. D. (1997). Identification and expression of *uvi31*$^+$, a UV-inducible gene from *Schizosaccharomyces pombe*. Environ. Mol. Mutagen *30*, 72–81.

Krien, M.J.E., West, R. R., John, U. P., Koniaras, K., McIntosh, J. R., and O'Connell, M. J. (2002). The fission yeast NIMA kinase Fin1p is required for spindle function and nuclear envelope integrity. EMBO J. *21*, 1713–1722.

Lin, K., Liu, J., Miller, D. L., and Wong, L. (2004). Genome-wide cDNA oligo design and its applications in *Schizosaccharomyces pombe*. In: The Practical Bioinformatician, ed. L. Wong, Singapore: World Scientific Publishing, 347–358.

Lowndes, N. F., McInerny, C. J., Johnson, A. L., Fantes, P. A., and Johnston, L. H. (1992). Control of DNA synthesis genes in fission yeast by the cell-cycle gene *cdc10*$^+$. Nature *355*, 449–453.

Lydall, D., Ammerer, G., and Nasmyth, K. (1991). A new role for MCM1 in yeast: cell cycle regulation of *SW15*transcription. Genes Dev. *5*, 2405–2419.

MacNeill, S. A., and Fantes, P. A. (1997). Genetic and physiological analysis of DNA replication in fission yeast. Methods Enzymol. *283*, 440–459.

MacNeill, S. A., and Nurse, P. (1997). Cell cycle control in fission yeast. In: The Molecular and Cellular Biology of the Yeast *Saccharomyces*. Cell Cycle and Cell Biology, ed. J. R. Pringle, J. R. Broach, and E. W. Jones, Cold Spring Harbor, NY: Cold Spring Harbor Laboratory Press, 697–763.

Maqbool, Z., Kersey, P. J., Fantes, P. A., and McInerny, C. J. (2003). MCB-mediated regulation of cell cycle-specific *cdc22*$^+$transcription in fission yeast. Mol. Gen. Genomics *269*, 765–775.

Martín-Cuadrado, A. B., Dueñas, E., Sipiczki, M., Vázquez de Aldana, C. R., and del Rey, F. (2003). The endo-$\beta$-1,3-glucanase eng1p is required for dissolution of the primary septum during cell separation in *Schizosaccharomyces pombe*. J. Cell Sci. *116*, 1689–1698.

Matsumoto, S., and Yanagida, M. (1985). Histone gene organization of fission yeast: a common upstream sequence. EMBO J. *4*, 3531–3538.

McInerny, C. J., Kersey, P. J., Creanor, J., and Fantes, P. A. (1995). Positive and negative roles for *cdc10*in cell cycle gene expression. Nucleic Acids Res. *23*, 4761–4768.

Mitchison, J. M. (1970). Physiological and cytological methods for *Schizosaccharomyces pombe*. Methods Cell Physiol. *4*, 131–165.

Mitchison, J. M., Creanor, J., and Novak, B. (1991). Coordination of growth and division during the cell cycle of fission yeast. Cold Spring Harbor Symp. Quant. Biol. *56*, 557–565.

Miyamoto, M., Tanaka, K., and Okayama, H. (1994). res2$^+$, a new member of the *cdc10*$^+$*/SWI4* family, controls the "start" of mitotic and meiotic cycles in fission yeast. EMBO J. *13*, 1873–1880.

Muzi-Falconi, M., and Kelly, T. J. (1995). Orp1, a member of the Cdc18/Cdc6 family of S-phase regulators, is homologous to a component of the origin recognition complex. Proc. Natl. Acad. Sci. USA *92*, 12475–12479.

Nakashima, N., Tanaka, K., Sturm, S., and Okayama, H. (1995). Fission yeast Rep2 is a putative transcriptional activator subunit for the cell cycle "start" function of Res2-Cdc10. EMBO J. *14*, 4794–4802.

Nasmyth, K., Nurse, P., and Fraser, R.S.S. (1979). The effect of cell mass on the cell cycle timing and duration of S-phase in fission yeast. J. Cell Sci. *39*, 215–233.

Ng, S. S., Anderson, M., White, S., and McInerny, C. J. (2001). mik1$^+$G1-S transcription regulates mitotic entry in fission yeast. FEBS Lett. *503*, 131–134.

Nurse, P. (1990). Universal control mechanism regulating onset of M-phase. Nature *344*, 503–508.

Obara-Ishihara, T., and Okayama, H. (1994). A B-type cyclin negatively regulates conjugation via interacting with cell cycle 'start' genes in fission yeast. EMBO J. *13*, 1863–1872.

Ohkura, H., and Yanagida, M. (1991). *S. pombe* gene *sds22*$^+$essential for a midmitotic transition encodes a leucine-rich repeat protein that positively modulates protein phosphatase-1. Cell *64*, 149–157.

Plochocka-Zulinska, D., Rasmussen, G., and Rasmussen, C. (1995). Regulation of calcineurin gene expression in *Schizosaccharomyces pombe*. Dependence on the *ste11* transcription factor. J. Biol. Chem. *270*, 24794–24799.

Rasmussen, C. D. (2000). Cloning of a calmodulin kinase I homologue from *Schizosaccharomyces pombe*. J. Biol. Chem. *275*, 685–690.

Reymond, A., Schmidt, S., and Simanis, V. (1992). Mutations in the *cdc10*start gene of *Schizosaccharomyces pombe* implicate the region of homology between *cdc10*and *S.W.I6*as important for p85$^{cdc10}$function. Mol. Gen. Genet. *234*, 449–456.

Ribár, B., Bánrévi, A., and Sipiczki, M. (1997). sep1$^+$encodes a transcription-factor homologue of the HNF-3/forkhead DNA-binding-domain family in *Schizosaccharomyces pombe*. Gene *202*, 1–5.

Ribár, B., Grallert, A., Oláh, É., and Szállási, Z. (1999). Deletion of the *sep1*$^+$forkhead transcription factor homologue is not lethal but causes hyphal growth in *Schizosaccharomyces pombe*. Biochem. Biophys. Res. Commun. *263*, 465–474.

Rifkin, S. A., and Kim, J. (2002). Geometry of gene expression dynamics. Bioinformatics *18*, 1176–1183.

Robinow, C. F. (1977). The number of chromosomes in *Schizosaccharomyces pombe*: light microscopy of stained preparations. Genetics *87*, 491–497.

Rowley, R., Hudson, J., and Young, P. G. (1992). The *wee1*protein kinase is required for radiation-induced mitotic delay. Nature *356*, 353–355.

Russell, P., and Nurse, P. (1986). cdc25$^+$functions as an inducer in the mitotic control of fission yeast. Cell *45*, 145–153.

Rustici, G., Mata, J., Kivinen, K., Lió, P., Penkett, C. J., Burns, G., Hayles, J., Brazma, A., Nurse, P., and Bähler, J. (2004). Periodic gene expression program of the fission yeast cell cycle. Nat. Genet. *36*, 809–817.

Samuel, J. M., Fournier, N., Simanis, V., and Millar, J.B.A. (2000). spo12 is a multicopy suppressor of *mcs3*that is periodically expressed in fission yeast mitosis. Mol. Gen. Genet. *264*, 306–316.

Sellers, J. W., Vincent, A. C., and Struhl, K. (1990). Mutations that define the optimal half-site for binding yeast GCN4 activator protein and identify an ATF/CREB-like repressor that recognizes similar DNA sites. Mol. Cell. Biol. *10*, 5077–5086.

Simon, I., *et al*. (2001). Serial regulation of transcriptional regulators in the yeast cell cycle. Cell *106*, 697–708.

Spellman, P. T., Sherlock, G., Zhang, M. Q., Iyer, V. R., Anders, K., Eisen, M. B., Brown, P. O., Botstein, D., and Futcher, B. (1998). Comprehensive identification of cell cycle-regulated genes of the yeast *Saccharomyces cerevisiae* by microarray hybridization. Mol. Biol. Cell *9*, 3273–3297.

Sugiyama, A., Tanaka, K., Okazaki, K., Nojima, H., and Okayama, H. (1994). A zinc finger protein controls the onset of premeiotic DNA synthesis of fission yeast in a Mei2-independent cascade. EMBO J. *13*, 1881–1887.

Takahashi, K., Chen, E. S., and Yanagida, M. (2000). Requirement of Mis6 centromere connector for localizing a CENP-A-like protein in fission yeast. Science *288*, 2215–2219.

Takeda, T., Ogino, K., Matsui, E., Cho, M. K., Kumagai, H., Miyake, T., Arai, K.-I., and Masai, H. (1999). A fission yeast gene, him1$^+$/dfp1$^+$, encoding a regulatory subunit for Hsk1 kinase, plays essential roles in S-phase initiation as well as in S-phase checkpoint control and recovery from DNA damage. Mol. Cell. Biol. *19*, 5535–5547.

Tanaka, H., Ryu, G.-H., Seo, Y.-S., Tanaka, K., Okayama, H., MacNeill, S. A., and Yuasa, Y. (2002). The fission yeast *pfh1*$^+$ gene encodes an essential 5′ to 3′ DNA helicase required for the completion of S-phase. Nucleic Acids Res. *30*, 4728–4739.

Tanaka, K., and Russell, P. (2001). Mrc1 channels the DNA replication arrest signal to checkpoint kinase Cds1. Nat. Cell Biol. *3*, 966–972.

Tang, H., and Lewontin, R. C. (1999). Locating regions of differential variability in DNA and protein sequences. Genetics *153*, 485–495.

Tournier, S., and Millar, J.B.A. (2000). A role for the START gene-specific transcription factor complex in the inactivation of cyclin B and Cut2 destruction. Mol. Biol. Cell *11*, 3411–3424.

White, S., Khaliq, F., Sotiriou, S., and McInerny, C. J. (2001). The role of DSC1 components *cdc10*$^+$, rep1$^+$and rep2$^+$in MCB gene transcription at the mitotic G1-S boundary in fission yeast. Curr. Genet. *40*, 251–259.

Whitehall, S., Stacey, P., Dawson, K., and Jones, N. (1999). Cell cycle-regulated transcription in fission yeast: Cdc10-Res protein interactions during the cell cycle and domains required for regulated transcription. Mol. Biol. Cell *10*, 3705–3715.

Whitfield, M. L., *et al*. (2002). Identification of genes periodically expressed in the human cell cycle and their expression in tumors. Mol. Biol. Cell *13*, 1977–2000.

Wood, V., *et al*.(2002). The genome sequence of *Schizosaccharomyces pombe*. Nature *415*, 871–880.

Yamada, H. Y., Matsumoto, S., and Matsumoto, T. (2000). High dosage expression of a zinc finger protein, Grt1, suppresses a mutant of fission yeast *slp1*$^+$, a homolog of CDC20/p55CDC/Fizzy. J. Cell Sci. *113*, 3989–3999.

Yamaguchi, S., Okayama, H., and Nurse, P. (2000). Fission yeast Fizzy-related protein srw1p is a $G_1$-specific promoter of mitotic cyclin B degradation. EMBO J. *19*, 3968–3977.

Zhu, Y., Takeda, T., Nasmyth, K., and Jones, N. (1994). pct1$^+$, which encodes a new DNA-binding partner of p85$^{cdc10}$, is required for meiosis in the fission yeast *Schizosaccharomyces pombe*. Genes Dev. *8*, 885–898.

Zilahi, E., Salimova, E., Simanis, V., and Sipiczki, M. (2000). The *S. pombe sep1*gene encodes a nuclear protein that is required for periodic expression of the *cdc15* gene. FEBS Lett. *481*, 105–108.